Available online at www.sciencedirect.com
SCIENCE DIRECT®
ELSEVIER
Palaeogeography, Palaeoclimatology, Palaeoecology 207 (2004) 203–237
PALAEO
www.elsevier.com/locate/palaeo

Late Oligocene bunch grassland and early Miocene sod grassland paleosols from central Oregon, USA

Gregory J. Retallack*

Department of Geological Sciences, University of Oregon, Eugene, OR 97403-1272, USA

Received 4 March 2002; accepted 25 September 2003

Abstract

Fossil soils, burrows and mammals of the upper John Day Formation in central Oregon are evidence of bunch grasses and open, semiarid vegetation as old as late Oligocene (earliest Arikareean, 30 Ma). Root traces in these paleosols include both stout, tapering tubes, like roots of trees, as well as sinuous filamentous tubes, similar to roots of grasses. Paleosol structure is fine subangular blocky, with patchy distribution of grass-like roots, as in wooded grassland and sagebrush steppe with bunch grasses. Cursoriality in horses (*Mesohippus*, *Miohippus*) and hypsodonty in rhinos (*Diceratherium*) is also evidence for open grassy vegetation. Trace fossils of *Pallichnus* (dung beetle boli) and *Edaphichnium* (earthworm chimneys) are characteristic of wooded grassland paleosols, whereas *Taenidium* (cicada burrows) dominates desert shrubland paleosols, as has also been found in Quaternary paleosols and soils of eastern Washington. In both Oligocene and Quaternary paleosol sequences, arid shrubland and semiarid grassland paleosols alternate on Milankovitch frequencies (23, 41, 100 ka).

The oldest known paleosols in Oregon with crumb structure and abundant fine fossil root traces characteristic of sod grasslands are dated by mammalian biostratigraphy as Hemingfordian (early Miocene, ca. 19 Ma). Wooded grassland habitats are indicated by scattered chalcedony-calcite rhizoconcretions from large woody plants, and by fossil chalicotheres (*Moropus*), camels (*Gentilicamelus*, "*Paratylopus*") and horses (*Parahippus*). Silty texture and silcrete horizons are evidence of semiarid to arid paleoclimate, and are in striking contrast to highly calcareous, and clayey underlying paleosols of the John Day Formation. These silcrete paleosols may represent the Miocene onset of summer-dry (Mediterranean) seasonality, as opposed to a summer-wet (monsoonal) pattern of seasonality found in this region during the Oligocene.

Oregon's early rangelands can be compared with those in the North American Great Plains. Granular-structured calcareous paleosols of the Brule Formation of South Dakota are evidence of dry, bunch grasslands as old as 33 Ma (early Orellan, early Oligocene), and crumb-structured paleosols of the Anderson Ranch Formation of Nebraska are evidence of sod grasslands as old as 19 Ma (late Arikareean, early Miocene). Although grasses were a conspicuous part of dry rangelands well back into the Oligocene, early and middle Miocene sod grasslands in North America were restricted to regions estimated to have had less than 400 mm mean annual precipitation.
© 2004 Elsevier B.V. All rights reserved.

Keywords: Grassland; Paleosol; Trace fossil; Fossil mammal; Oligocene; Miocene

1. Introduction

The antiquity of grasslands has been of interest ever since Darwin (1872) suggested its role in

* Tel.: +1-541-3464558; fax: +1-541-3464692.
E-mail address: gregr@darkwing.uoregon.edu (G.J. Retallack).

0031-0182/$ - see front matter © 2004 Elsevier B.V. All rights reserved.
doi:10.1016/j.palaeo.2003.09.027

human evolution and since Kowalevsky (1873) demonstrated the profound influence of grasslands on the evolution of horses and other ungulates. Mammalian hypsodonty is still regarded as an adaptation to abrasiveness of grassy diet and mammalian cursorality as an adaptation to open vegetation (Janis, 2000; Janis et al., 2002), but various components of grasslands ecosystems evolved at different times. Cursoriality appears in the North American fossil mammal record by early Oligocene (33 Ma), and hypsodonty by early Miocene (18 Ma), but large, highly hypsodont, fully cursorial horses do not appear until late Miocene (7 Ma: MacFadden, 2000). Molecular clock studies of artiodactyl digestive RNases indicate an origin for ruminant grass-digesting enzymes in the late Eocene to early Oligocene (Jermann et al., 1995). Microwear studies indicate a significant intake of grass by Oligocene horses, but some Miocene horses were true grazers (Solounias and Semprebon, 2002). Isotopic studies of Miocene fossil grasses and hypsodont mammals indicate that most grasses in tropical regions then were C_3 plants, as is typical today only of high latitude and high altitude grasses, and of most trees and shrubs (Koch, 1998; MacFadden, 2000). Carbon isotopic composition of fossil tooth enamel and paleosol carbonate nodules indicate small amounts (20%) of C_4 grasses or CAM plants at least from the mid-Oligocene (29 Ma: Retallack, 2002a; Fox and Koch, 2003), and perhaps earlier (Wang and Cerling, 1994), but a marked late Miocene–Pliocene (7–2.5 Ma) increase in abundance of C_4 grasses throughout tropical regions (Cerling et al., 1997; Fox and Koch, 2003, this volume). The fossil record of grass leaves, anthoecia, pollen and phytoliths reveal grasses well back into the Eocene, but widespread taxa of open grasslands no earlier than late Oligocene (Dugas and Retallack, 1993; Morley and Richards, 1993; Jacobs et al., 1999; Strömberg, 2002, this volume). Another record of past grasslands with high temporal resolution is now becoming available from the study of paleosols which reveal for the Great Plains of North America a three-stage evolution of Oligocene (33 Ma) desert bunch grasslands, early Miocene (19 Ma) short sod grasslands and late Miocene (7 Ma) tall sod grasslands (Retallack, 1997a, 2001a; Retallack et al., 2002; with revised dating by MacFadden and Hunt, 1998). This study documents the paleosol record of late Oligocene bunch grassland and early Miocene sod grassland ecosystems in central Oregon (Figs. 1 and 2).

Paleosols of sod grasslands have abundant, filamentous (less than 2 mm diameter), fossil root holes and common, rounded pellets of earthworms and other crumb peds. Soils with organically bound, stable structure and elevated organic content for at least 25 cm thickness are segregated as Mollisols in the US soil taxonomy (Soil Survey Staff, 1999) or as Chernozems in the FAO (1974) and other classifications (Stace et al., 1968). Soil organic matter, actual roots and other body fossils of grasses are seldom preserved in grassland paleosols because grasslands, as opposed to marshes and fens, are well drained and oxidized, allowing organic matter decay even after burial (Retallack, 1998). Plant opal (phytoliths) accumulates in soils and is locally abundant in paleosols as an additional line of evidence for grasses (Strömberg, 2002, this volume), but the distinction between sod and bunch grassland is not easily inferred from phytoliths. Nor is this distinction apparent from carbon isotopic detection of C_4 grasses, which form both sod and bunch grasslands in regions with warm growing season. Furthermore, C_4 grasses never spread into Oregon (Cerling et al., 1997). Other trace fossils in paleosols indicative of grasslands include the chimneys and fecal pellets of earthworms (*Edaphichnium*) and the boli and clayey shells of dung beetles (*Pallichnus*, *Coprinisphaera*: Retallack, 1990; Duringer et al., 2000; Genise et al., 2000). Earthworm fecal pellets in grassland paleosols are more common than isolated chimneys and burrow fills. They dominate the very fabric of grassland soils, which have, in effect, been through the guts of earthworms many times (Darwin, 1896). European earthworms are especially well known in this respect and have been widely exported for pasture improvement, but native earthworms of the New World, Asia and Australia also have comparable effects on soils (Joshi and Kelkar, 1952; Barley, 1959; Pawluk and Bal, 1985). These small 2–5 mm ellipsoidal fecal pellets are also comparable in size to the spacing of lateral rootlets on the filamentous roots of grasses (Weaver, 1920). Both grass roots and earthworms create in soils of sod grasslands a characteristic crumb ped structure, which

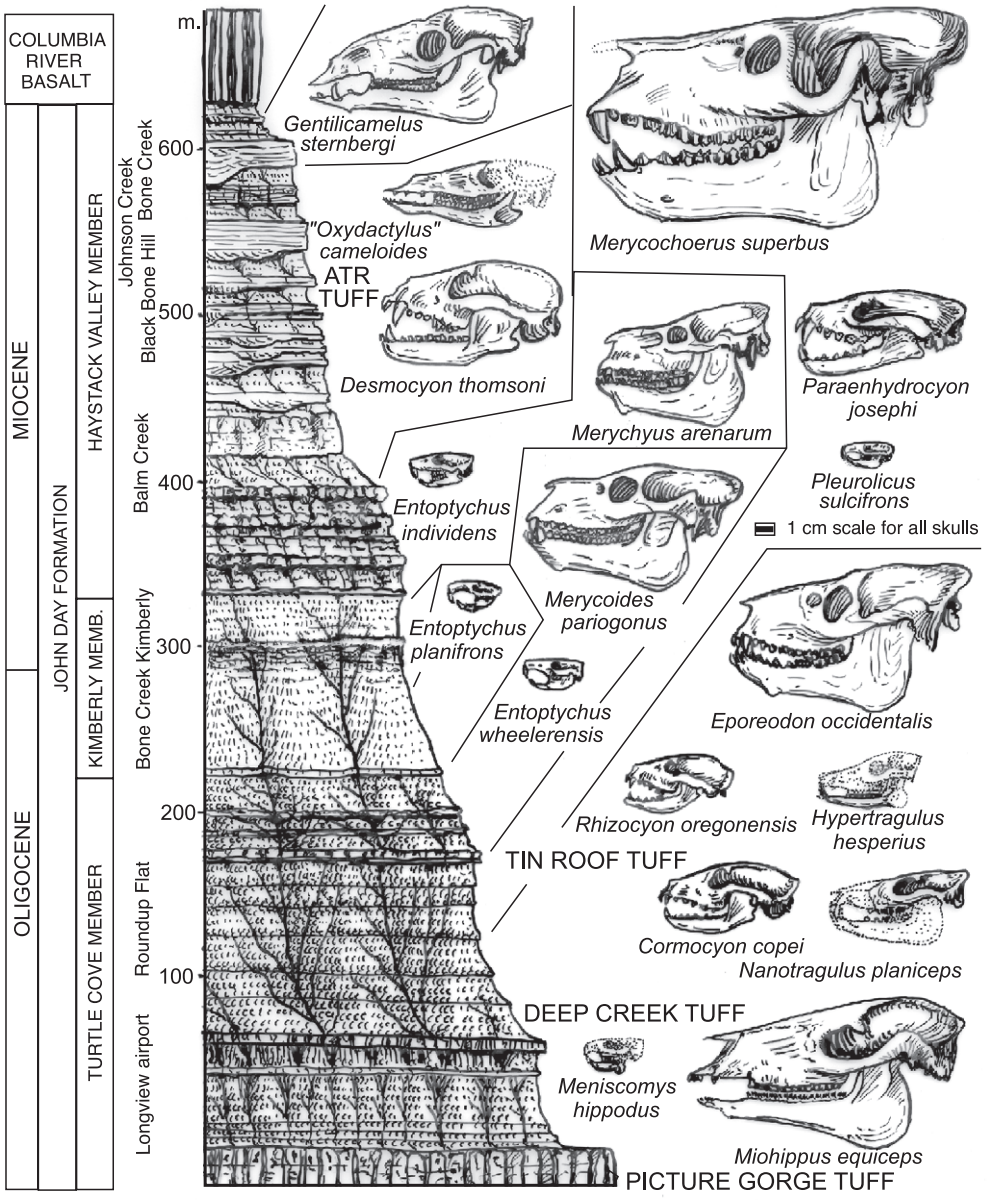

Fig. 1. Geological sequence and selected mammal fossils from the upper John Day Formation, near Kimberly, central Oregon (fossil illustrations after Sinclair, 1905; Osborn, 1918; Lull, 1921; Schultz and Falkenbach, 1947, 1949, 1968; Rensberger, 1971, 1983; Wang, 1994; Wang et al., 1999; Bryant, 1996; Prothero, 1996; Lander, 1998). Stippled portions of skulls are reconstructed, rather than preserved.

is commonly preserved in paleosols (Retallack, 1997a,b, 2001a). Other features of paleosols such as silcretes, calcareous nodules, chemical composition and grain size are indications of former climate, sedimentary setting, parent materials and duration of soil formation (Retallack, 2001b), and reveal the evolutionary and environmental context of early grassland ecosystems.

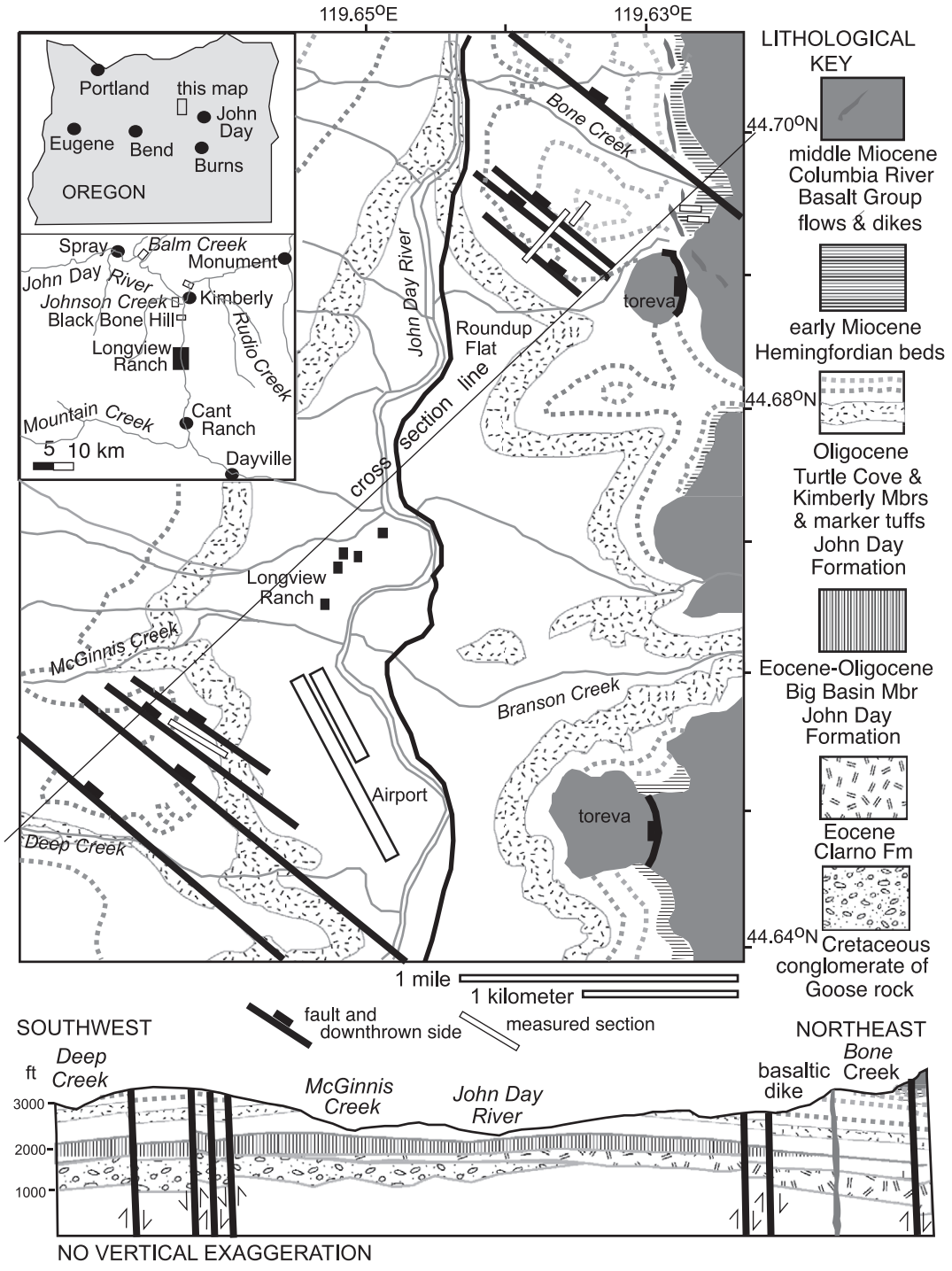

Fig. 2. Geological map and cross-section of Longview Ranch, south of Kimberly, central Oregon.

2. Materials and methods

2.1. Field and laboratory approaches

This research focused on measurement of detailed stratigraphic sections documenting every paleosol and its environmentally sensitive features in the late Oligocene to early Miocene upper John Day Formation near Kimberly and Spray, central Oregon (Figs. 1 and 2). All paleosols were logged using eye-heights at locations chosen so that a composite section could be assembled from the correlation of volcanic ash and other marker beds in three separate areas on Longview Ranch (Figs. 2–5) and four additional areas around Kimberly and Spray (Figs. 2, 6–8). Field measures taken were reaction with dilute acid (1.2 M HCl), Munsell color, depth to carbonate and assessment of the degree of development of the paleosols from carbonate nodule size and abundance, and from destruction of relict bedding (Retallack, 1997b). Selected profiles and specimens were analyzed for major oxides and trace elements by Bondar Clegg Inc of Vancouver BC (Appendix A), and selected molar weathering ratios were calculated (Retallack, 1997b). Carbonate nodules were analyzed for few of the paleosols, because this study aimed to quantify non-calcic hydrolysis. Petrographic thin sections were counted for 500 points in separate counts for mineral composition and grain size using a Swift automatic counter (Retallack, 2002a), with precision of about 2% (Murphy, 1983). These data

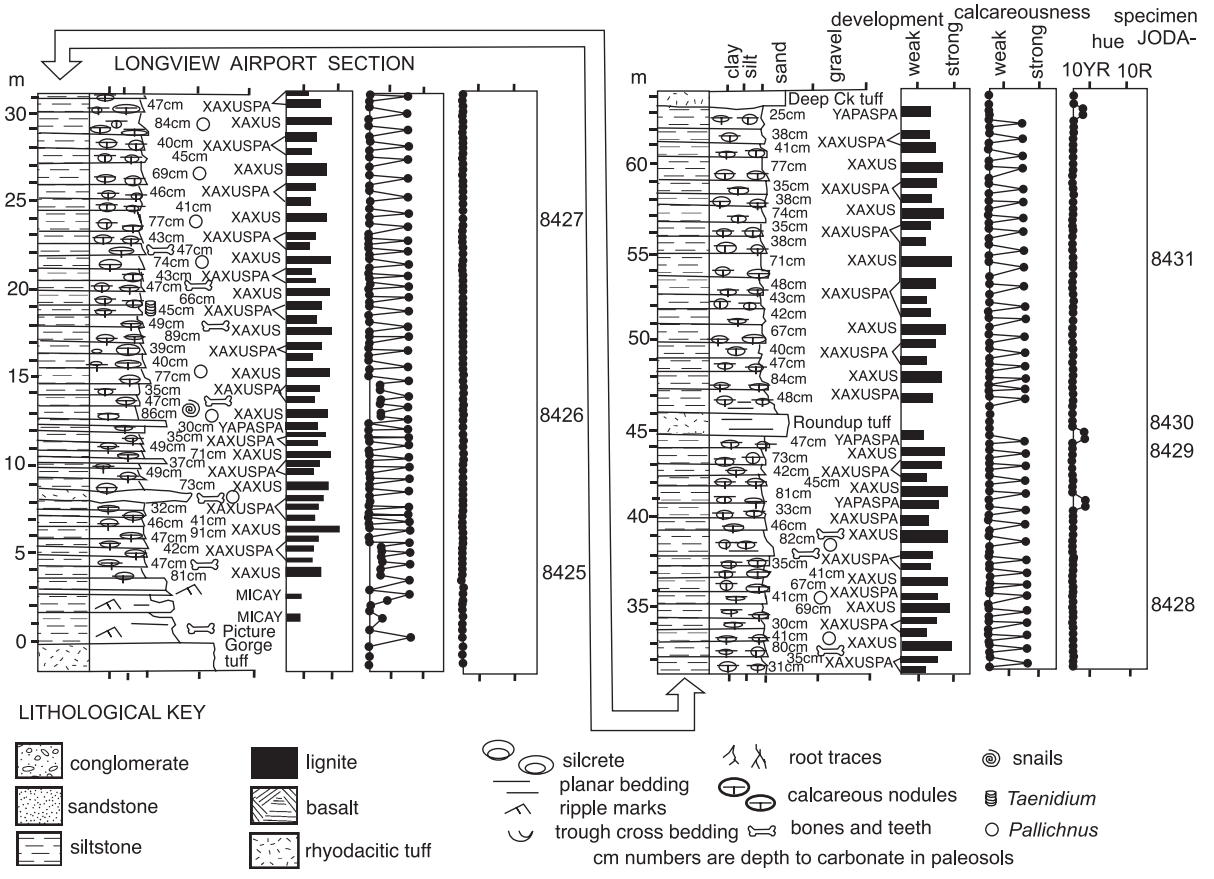

Fig. 3. Longview Ranch Airport section: a measured section showing degree of development (scale of Retallack, 1997b), calcareousness (reaction with 0.1 N HCl scale of Retallack, 1997b) and Munsell hue of paleosols of the middle Turtle Cove Member, John Day Formation in the badlands 1 km west of Longview Ranch airport (N44.663814° E119.66659°). JODA numbers refer to rock specimens curated at John Day Fossil beds national Monument, Kimberly, Oregon (catalog online http://www.museum.nps.gov).

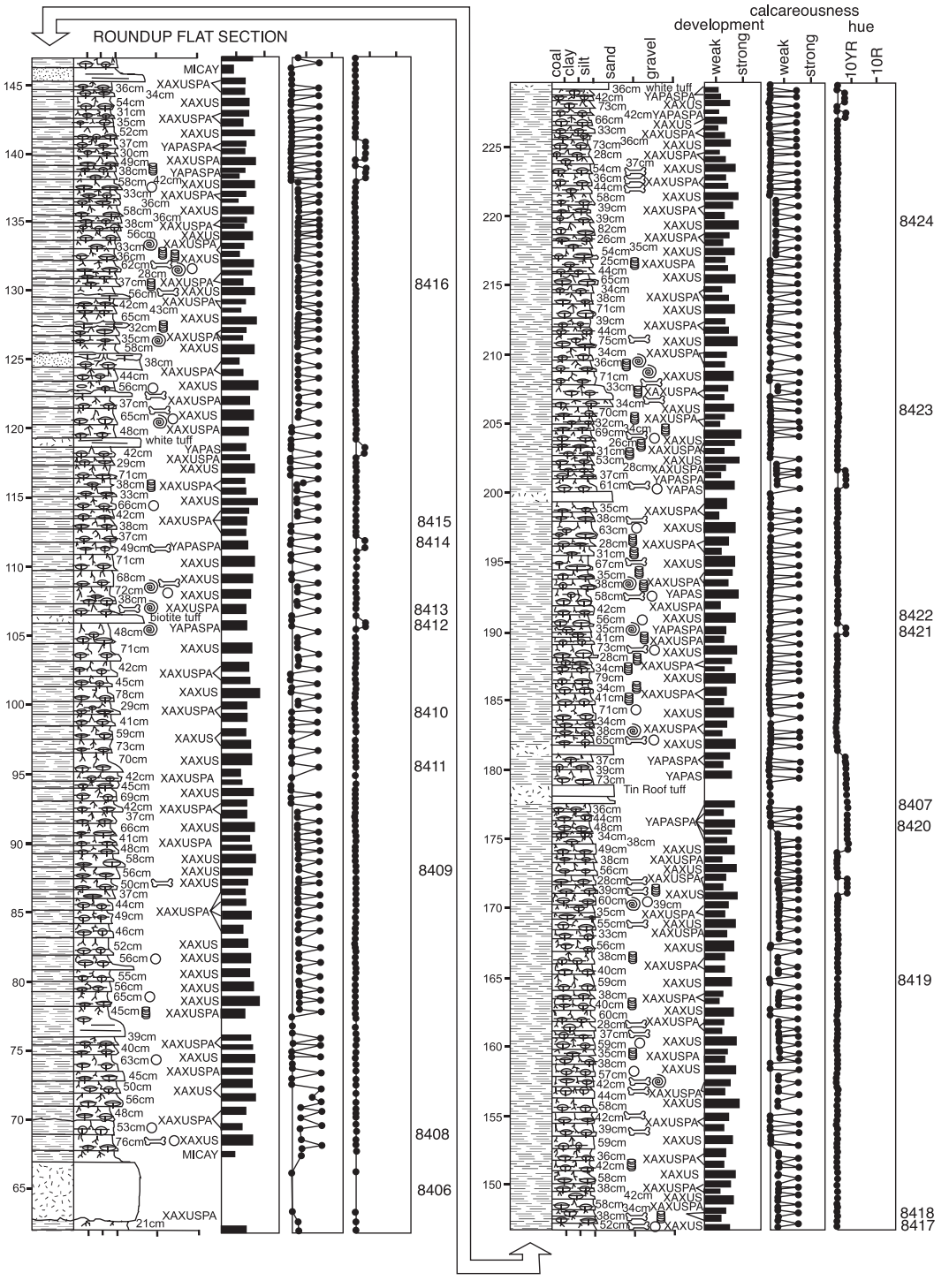

Fig. 4. Roundup Flat section: a measured section of paleosols of the upper Turtle Cove Member of the John Day Formation in the prominent badlands 2 km northeast of Longview Ranch (N44.692465° E119.638896°). The lithological key and conventions are as for Fig. 3.

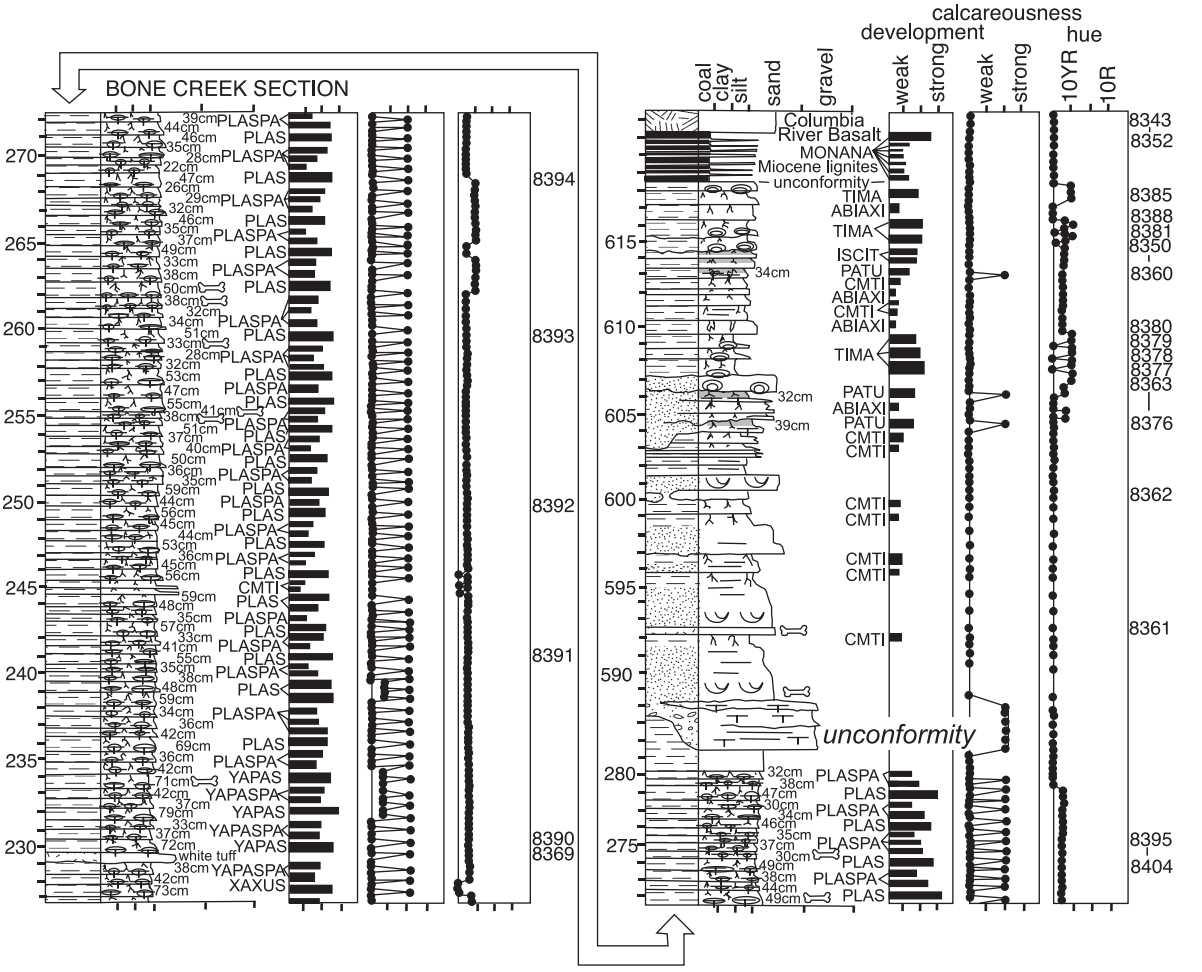

Fig. 5. Bone Creek Section: a measured section of paleosols of the uppermost Turtle Cove and Kimberly Members and Hemingfordian beds of the John Day Formation in gullies high within the headwaters of Bone Creek, 3 km northeast of Longview Ranch (N44.700229° E119.624658°). Lithological key and conventions are as for Fig. 3. Meter levels of the upper portion of this section are estimated from a regional composite stratigraphic section including strata missing in an erosional disconformity here.

supplement comparable data published elsewhere (Retallack et al., 2000). Descriptive terminology of the paleosols is after Brewer (1976) and Soil Survey Staff (1993). Rocks and fossils collected as a part of this work are curated at the John Day Fossil Beds National Monument, Kimberly (catalog online at http://www.museum.nps.gov).

2.2. Stratigraphic setting

The upper John Day Formation in the John Day Valley of central Oregon is well known for fossil mammals ranging in age from early Oligocene (fragmentary Orellan North American Land Mammal Age or NALMA, entelodons only) to early Miocene (Hemingfordian NALMA: Fremd et al., 1994; Orr and Orr, 1998; Coombs et al., 2001; Hunt and Stepleton, 2001). The upper Turtle Cove, Kimberly and lower Haystack Valley Members yield mammal fossils of the Arikareean NALMA (Fig. 9), and include the 'Monroecreekian' (29.5–25.8 Ma) and 'Harrisonian' (25.8–23.5) subdivisions of Alroy (2000). The age of the lower part of the sequence is well constrained by four $^{40}Ar/^{39}Ar$ single-crystal laser-fusion

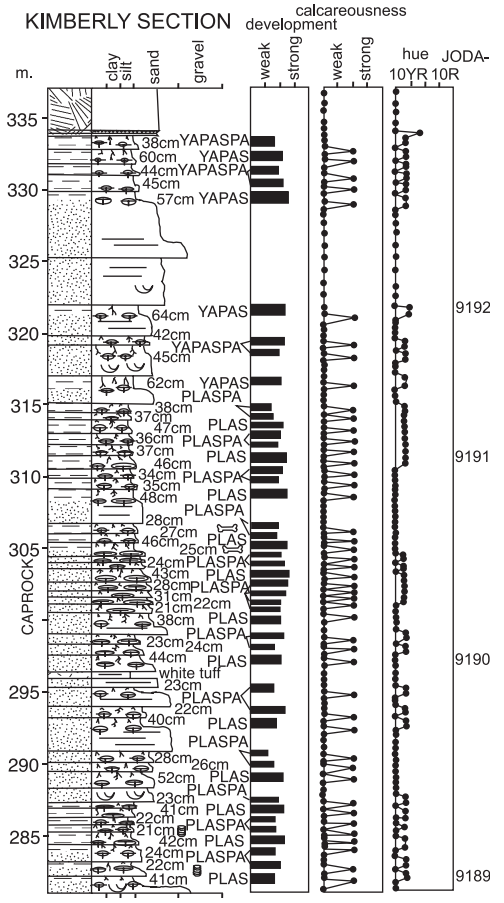

Fig. 6. Kimberly Section: a measured section of paleosols of the upper Kimberly Member of the John Day Formation in cliffs beside the road to Monument 1 km northeast of Kimberly (N44.776600° E119.630734°). The lithological key and conventions are as for Fig. 3.

radiometric ages on tuffs (by Swisher for Fremd et al., 1994), and by magnetostratigraphic chrons (Prothero and Rensberger, 1985; Albright et al., 2001), adjusted to the revised time scale of Cande and Kent (1992). The radiometric ages allow interpolation of geological age for the lower part of the sequence (black dots and regression line of Fig. 9), and give results not much different from the magnetostratigraphic chrons (also plotted in gray on Fig. 9). Dating of the upper part of the section is an extrapolation, supported by biostratigraphic correlations with Nebraska and one problematic radiometric age determination (Coombs et al., 2001).

Measured sections at Longview Ranch airport (Fig. 3), Roundup Flat (Fig. 4) and Bone Creek (Fig. 5) were correlated by means of the Deep Creek, Tin Roof and other marker tuffs (Fremd et al., 1994). They are also zoned biostratigraphically (Fig. 10), as the "*Promerycochoerus*" beds of Merriam and Sinclair (1906), and several rodent zones of *Meniscomys*, *Pleurolicus* and *Entoptychus* (Rensberger, 1971, 1973, 1983). The Kimberly Member, with *Entoptychus planifrons* at its base and *Entoptychus individens* at its top, is a distinctive loessic sequence of paleosols (Fig. 5) mappable from Bone Creek north to Kimberly (Fig. 6). The basal Haystack Creek Member near Balm Creek and Spray contains latest Arikareean mammals such as *E. individens* and *Merychyus arenarum*, and in the uppermost part of the exposures a tuff identified as the ATR tuff (Fig. 7). This tuff has been dated at Black Bone Hill (Fig. 8) as 22.6 Ma, which is an average of ages ranging from 24.4 to 19.6 Ma (Coombs et al., 2001). The tuff is redeposited and uncracked by soil formation, so that recycling of older grains is more likely than intrusion of younger grains. Other considerations favoring the youngest age includes paleomagnetic and radiometric dating of the basal Hemingfordian in Nebraska (MacFadden and Hunt, 1998), because the tuff at Black Bone Hill is 12 m above sites there for early Hemingfordian rodents *Schizodontomys greeni* and *Mylagaulodon angulatus* (Rensberger, 1973), as well as other mammals such as "*Paratylopus*" *cameloides* (Fremd et al., 1994; Honey et al., 1998). Overlying strata of the Johnson Creek and Bone Creek sections contain later Hemingfordian fossils including *Moropus oregonensis*, *Daphaenodon* sp., *Gentilicamelus sternbergi* and *Parahippus* sp. (Merriam and Sinclair, 1906; Woodburne and Robinson, 1977; Dingus, 1990; Honey et al., 1998; Lander, 1998; MacFadden, 1998; Hunt and Stepleton, 2001). This uppermost unit of the John Day Formation is unconformably overlain by basaltic sandstones and peaty paleosols of an unnamed unit with middle Miocene plant fossils, in turn, overlain by middle Miocene (16 Ma) Columbia River Basalt Group (Fisher and Rensberger, 1972). Disconformities due to paleovalley incision at the bottom and top of the Hemingfordian beds in upper Bone Creek (Fig. 5) have paleotopographic relief within the mapped area (Fig. 2) of at least 50 and 77 m, respectively. The lower disconformity was

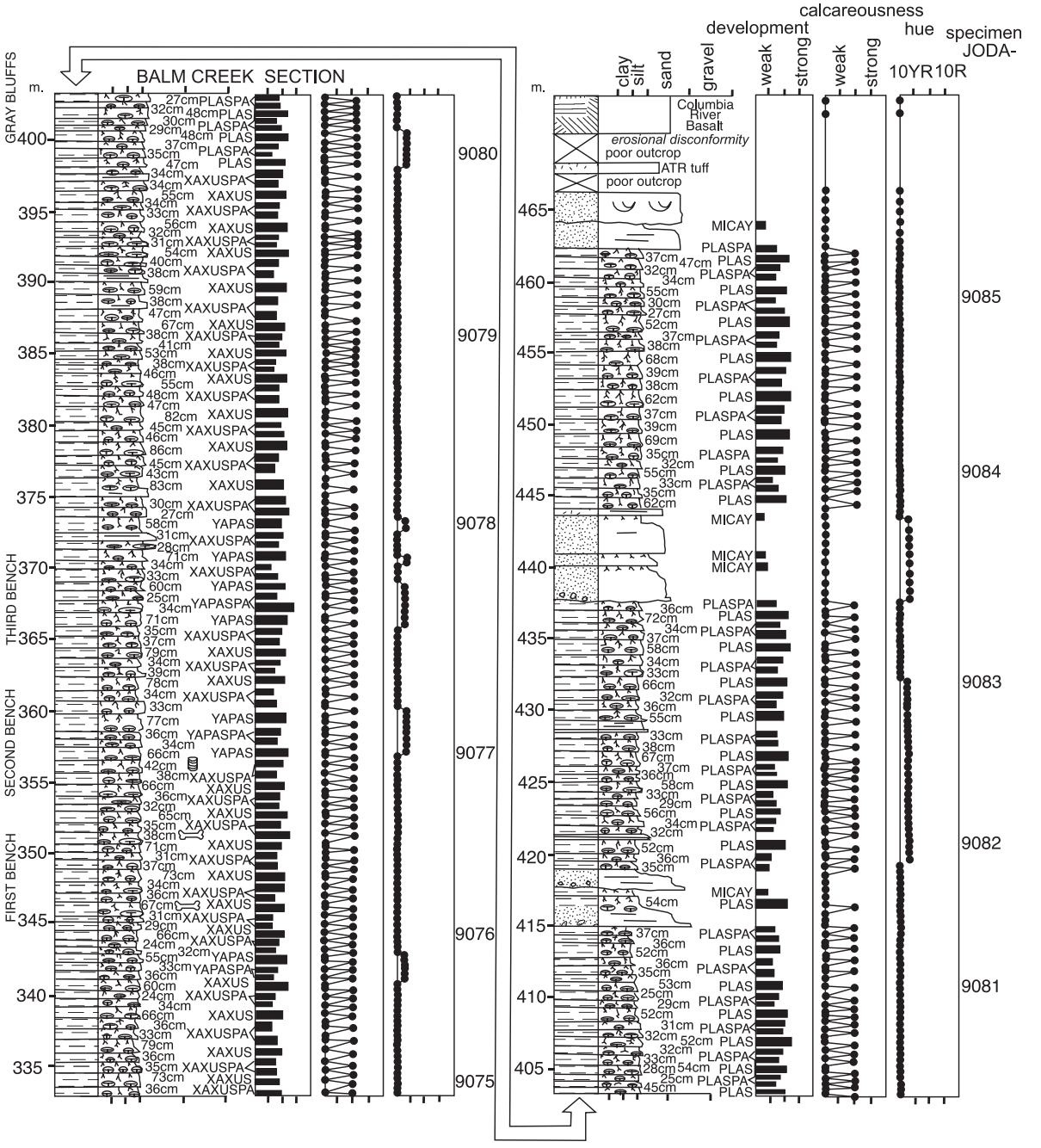

Fig. 7. Balm Creek Section: a measured section of paleosols of the lower Haystack Valley Member of the John Day Formation in badlands behind the house of Cal and Nina Hopper, east of Balm Creek, 3 km east of Spray (N44.837629° E119.740380°). The lithological key and conventions are as for Fig. 3.

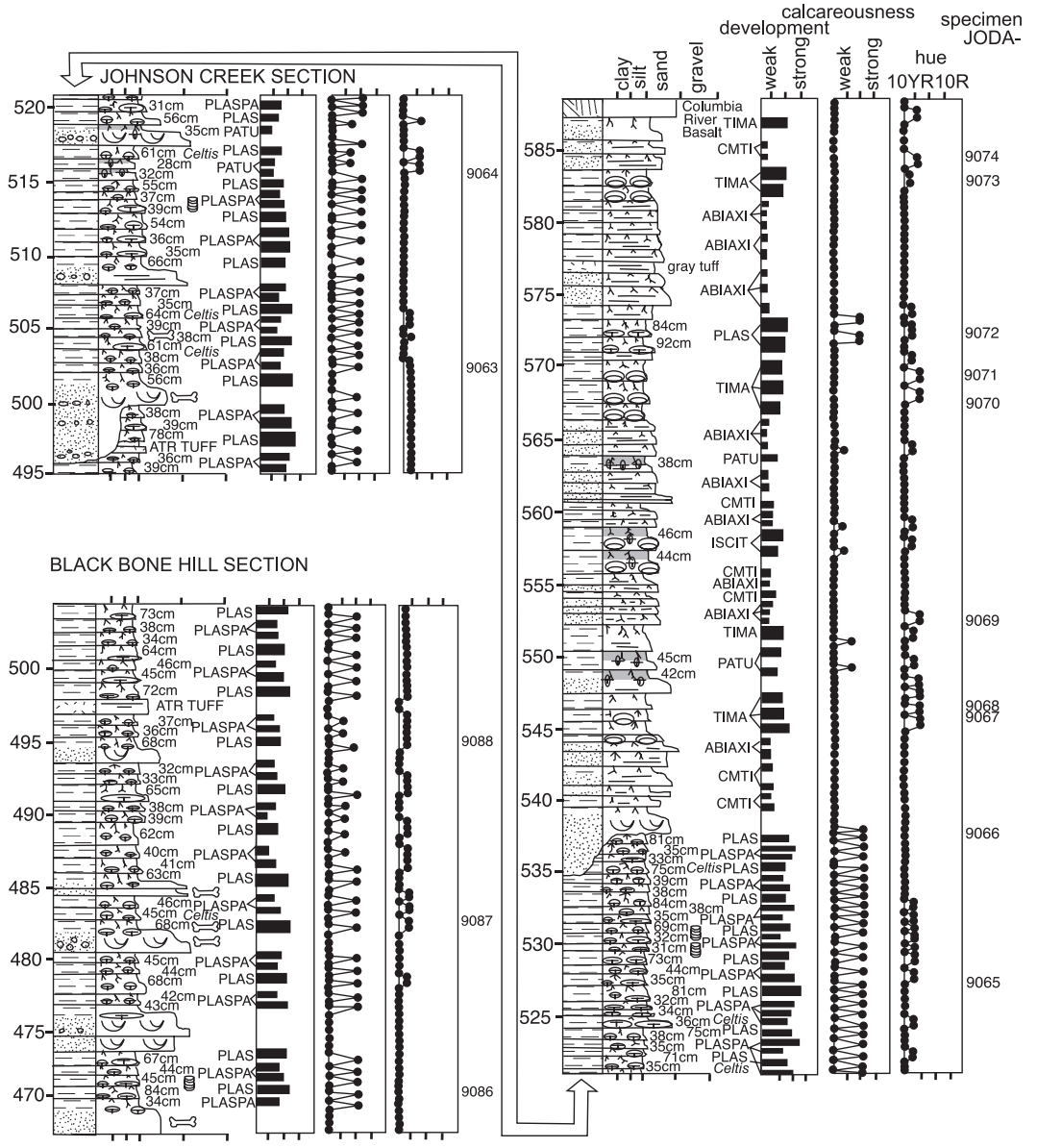

Fig. 8. Black Bone Hill and Johnson Creek Sections: a measured section of paleosols of the middle and upper Haystack Valley Member of the John Day Formation in a conical white hill west of the John Day River 1 km south of Kimberly (N44.74053° E119.647158°) and in cliffs north of the farm road into the canyon of Johnson Creek 1 km west of Kimberly (N44.752470° E119.654222°). The lithological key and conventions are as for Fig. 3.

filled by basal conglomerates with paleocurrents indicating that the paleovalley drained to the northwest, which is the same direction as flow within the much broader depositional basin of the Turtle Cove Member (Fig. 11).

2.3. Alterations after burial

Diagenetic alterations of paleosols of the John Day Formation have been discussed at length elsewhere (Retallack et al., 2000) and include burial gleization,

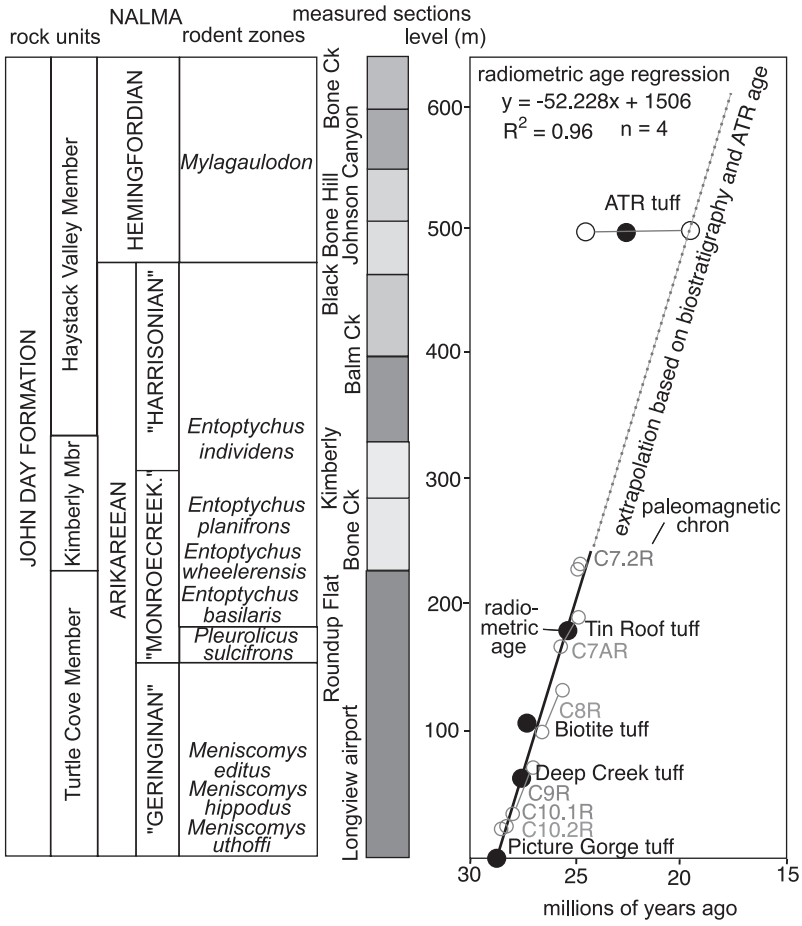

Fig. 9. Graphic correlation and regression of new $^{39}Ar/^{40}Ar$ ages (black circles) for tuffs in the upper John Day Formation on Longview Ranch (Fremd et al., 1994). Also shown (gray text) are magnetostratigraphic chrons (C10.2R to C7.2R after Prothero and Rensberger, 1985), and North American Land Mammal "Ages" (NALMA of Alroy, 2000), and rodent biostratigraphy of Rensberger (1971, 1973, 1983). The youngest of the averaged dates for the ATR tuff is most consistent with underlying Hemingfordian fossils (Coombs et al., 2001) and extrapolation from well-dated older rocks. The upper part of the succession is primarily dated by biostratigraphy.

celadonitization, zeolitization and burial compaction. The striking green color of the Turtle Cove Member and basal Haystack Valley Member in Balm Creek is from celadonite and clinoptilolite formed by Ostwald ripening of imogolite and illite during the early Miocene (Hay, 1963). Both the calcareous nodules and some paleosols (Yapas and Yapaspa pedotypes of Table 1) preserve light brown to gray colors that are probably close to original colors of the soils. The Kimberly Member and Hemingfordian parts of the Haystack Valley member are unzeolitized and unceladonitized (Hay, 1963), and their volcanic shards still glassy, so these paleosols also are more like the original soils. Lack of compactional deformation of volcanic shards in all these paleosols supports use of physical constants for Inceptisols in calculating burial compaction (Sheldon and Retallack, 2001).

3. Paleosol classification and its implications

3.1. Approaches to paleosol classitication

Paleosols of the upper John Day Formation are here classified using two quite different kinds of units: (1) field pedotypes and (2) taxonomic units. Pedo-

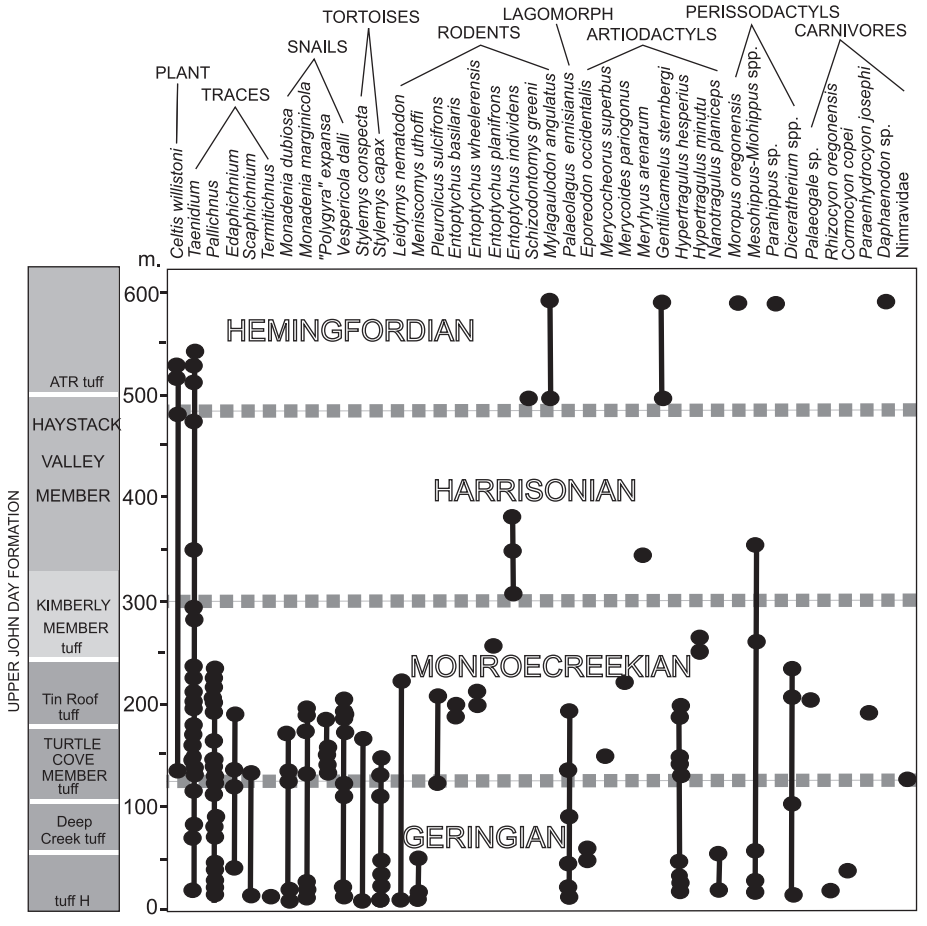

Fig. 10. Stratigraphic range of fossils collected during this study (all specimens curated in collections of John Day Fossil Beds National Monument: catalog online at http://www.museum.nps.gov).

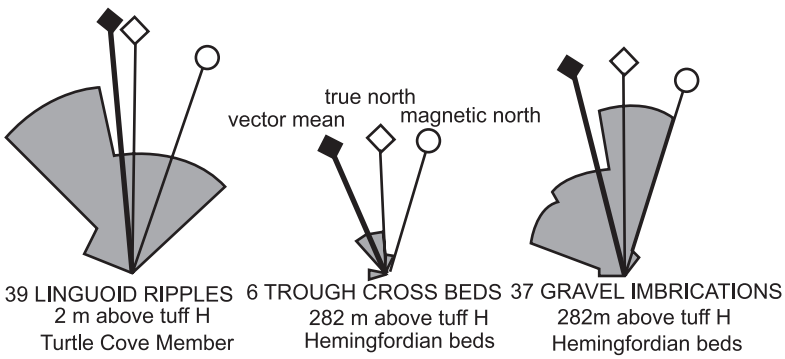

Fig. 11. Paleocurrents in the Turtle Cove Member and Hemingfordian beds of the John Day Formation.

Table 1
Inferred classification of reconstructed paleosols in the upper John Day Formation and lowermost Columbia River Basalt Group on Longview Ranch, central Oregon

Pedotype	Meaning	Type profile	Field diagnosis	US taxonomy	FAO map	Australian	Northcote key
Abiaxi	Bitter root	Bone Creek (299.0 m)	Chalcedony rhizoconcretions in high-soda clayey sandstone with relict bedding	Xerept	Eutric Cambisol	Brown clay	Uc1.21
Cmti (2)	New	Mascall Ranch	Brown siltstone with relict bedding and root traces	Fluvent	Eutric Fluvisol	Alluvial soil	Um1.21
Micay (1)	Root	Clarno mammal quarry	Brown to olive clay with root traces and relict bedding	Aquandic Fluvaquent	Eutric Fluvisol	Alluvial soil	Uf1.41
Iscit	Path	Bone Creek (310.0 m)	Crumb-structured surface (A) over thick siliceous duripan (Bq)	Durixeroll	Mollic Solonchak	Brown hardpan soil	Um6.22
Monana	Underneath	Bone Creek (317.3 m)	Clayey lignite (O) over basaltic sandstone (A)	Saprist	Histosol	Acid peat	O
Patu	Mountain	Bone Creek (302.4 m)	Crumb structured surface (A) over shallow (<50 cm) micrite-chalcedony rhizoconcretions (Bk)	Xeroll	Kastan-ozem	Cherno-zem	Um6.22
Plas	White	Bone Creek (275.5 m)	Silty white surface (A) with calcareous nodules (Bk)>45 cm deep	Typic Haplocalcid	Calcic Xerosol	Gray-brown calcareous soil	Gc1.21
Plaspa	In white	Bone Creek (275.8 m)	Silty white surface (A) with calcareous nodules (Bk)<45 cm deep	Ustic Haplocalcid	Calcic Yermisol	Gray-brown calcareous soil	Gc1.12
Tima	Write	Bone Creek (314.0 m)	Granular structured surface (A) over clayey subsurface (Bt) and siliceous duripan (Bq)	Natric Durixeralf	Mollic Solonetz	Solonetz	Dy4.13
Yapas (1)	Grease	Carroll Rim	Dark brown, fine blocky peds (A, Bw), calcareous nodules (Bk)>50 cm deep	Haplustand	Mollic Andosol	Prairie soil	Gc2.21
Yapaspa	In grease	Bone Creek (231.0 m)	Dark brown, fine blocky peds (A, Bw), calcareous nodules (Bk)<50 cm deep	Vitrandic Haplocalcid	Calcic Xerosol	Gray-brown calcareous soil	Gc2.12
Xaxus (1)	Green	Foree	Green, fine blocky peds (A, Bw), calcareous nodules (Bk)>50 cm deep	Aquic Ustivitrand	Vitric Andosol	Wiesen-boden	Gc1.21
Xaxuspa	In green	Foree (250 m)	Green, fine blocky peds (A, Bw), calcareous nodules (Bk)< 50 cm deep	Aquic Haplo-calcid	Calcaric Gleysol	Gray-brown calcareous soil	Gc1.12

Sahaptin meaning is after Rigsby (1965) and DeLancey et al. (1988): type profiles of most paleosols are described here, and the others are described by (1) Retallack et al. (2000), and (2) Retallack et al. (2002).

types are a non-genetic field mapping designation (Retallack, 1994a), comparable to soil series (Soil Survey Staff, 1993). These named pedotypes (Table 1) are part of a wider scheme of field mapping categories for paleosols in the John Day Formation (Retallack et al., 2000), using simple descriptive terms from the Sahaptin Native American language (Rigsby, 1965; DeLancey et al., 1988). Selected profiles of each pedotype not described elsewhere (Retallack et al., 2000) are characterized chemically and petrographically here (Table 2; Figs. 12–15). The Monana pedotype, logged and characterized during this study (Table 1; Fig. 5) is one of a variety of paleosols associated with the middle Miocene, Columbia River Basalt Group, rather than the John Day Formation. Paleosols of the John Day Formation formerly regarded as shallow-calcic variants of Xaxus, Yapas and Plas pedotypes (Retallack et al., 2000) are here

Table 2
Type sections of newly proposed pedotypes in upper Bone Creek section (Fig. 4) and Foree section (Xaxuspa only)

Paleosol	Level	A horizon	B horizon	C horizon
Type Abiaxi loam	299.0 m	0 cm, A, medium-grained sandstone, pale yellow (5Y7/3) with mottles up to 1 cm of light yellowish brown (2.5Y6/3); root traces woody and up to 3 mm diameter, replaced by chalcedony of white (5Y8/1) and clay of brown; non-calcareous; intertextic insepic microfabric, with common volcanic rock fragments	Not present	−68 cm, C, medium-grained sandstone light brownish gray (2.5Y6/3), with stringers of ripple-marked silty sandstone, white (5Y8/1); claystone clasts up to 5 mm of pale brown (10YR6/3); intertextic insepic microfabric, with common volcanic rock fragments
Type Iscit clay	310.0 m	0 cm, A, siltstone, light yellowish brown (2.5Y6/4); crumb peds with abundant fine (1–2 mm) root traces, and scattered large root traces (6–7 mm) of pale yellow (2.5Y8/2); non-calcareous; scattered clasts up to 4 mm of pale yellow (2.5Y8/2) and light olive brown (2.5Y5/6); pyrolusite dendrites black (5Y2.5/); insepic agglomeroplasmic, with rounded and coated grains	−15 cm, By, silicified medium-grained sandstone, light olive brown (2.5Y5/4), with mottles of pale yellow (2.5Y7/4), clay skins of grayish brown (2.5Y5/2), and granules of white (2.5Y8/1) and pale yellow (2.5Y8/3); scattered mangans (dark gray (2.5Y4/1); non-calcareous; insepic agglomeroplasmic, with rounded and coated grains	−45 cm (A horizon of Patu paleosol), light olive brown (2.5Y5/3), crumb peds, outlined by argillans of grayish brown (2.5Y5/2); root traces mostly fine (1 mm) but one was 8 cm diameter at a depth of 30 cm and expanded to 13 cm diameter at the surface; rare burrows 3 cm diameter filled with pale yellow (2.5Y7/3) sandstone; insepic intertextic
Type Patu clay loam	302.4 m	0 cm, A, siltstone, light yellowish brown (2.5Y6/3), crumb peds defined by argillans light olive brown (2.5Y5/3), abundant fine (1 mm) root traces of light olive brown (2.5Y5/3) and scattered large (4 mm) chalcedony rhizoconcretions of white (5Y8/1); scattered pyrolusite dendrites black (5Y2.5/1); non-calcareous; porphyroskelic skelmosepic, with concentrically banded rhizoconcretions	−32 cm, Bk, sandy siltstone, pale yellow (2.5Y7/3); weakly calcareous chalcedony rhizoconcretions of white (2.5Y8/1); few burrows 1.5 cm diameter of white (2.5Y8/1) sand; porphyroskelic mosepic in matrix, and calciasepic to insepic in banded rhizoconcretions	−41 cm, C, tuffaceous medium-grained sandstone, white (5Y8/1); non-calcareous, relict planar bedding; few large strata-concordant root traces 7 mm diameter of pale olive (5Y6/3) claystone; insepic agglomeroplasmic, with common rounded and coated soil granules
Type Plas clay	275.5 m	0 cm, A, clayey fine-grained sandstone, pale yellow (2.5Y7/3), non-calcareous; grains of white (2.5Y8/1) and olive gray (5Y4/2); abundant fine (1–2 mm) root traces of light olive brown (2.5Y3/3); insepic agglomeroplasmic microfabric, with common volcanic rock fragments and few shards	−62 cm, Bw, clayey fine-grained sandstone, light yellowish brown (2.5Y6/3); massive, non-calcareous; intertextic insepic −94 cm, Bk, large (up to 25 cm) calcareous nodules and ledges, gray (5Y5/1); moderately calcareous; few slickensided mangans very dark gray (5Y3/1); intertextic calciasepic	−118 cm (A horizon of Plaspa paleosol), clayey, fine –grained tuffaceous sandstone, pale yellow (2.5Y7/3), with root traces up to 4 mm diameter of light olive brown (2.5Y5/3); non-calcareous; agglomero-plasmic insepic microfabric

Table 2 (*continued*)

Paleosol	Level	A horizon	B horizon	C horizon
Type Plaspa clay loam	275.8 m	0 cm, A, clayey fine-grained tuffaceous sandstone, pale yellow (2.5Y7/3); with root traces up to 6 mm diameter of light olive brown (2.5Y5/3) and near-vertical burrow 2.4 cm diameter extending down 16 cm from surface; non-calcareous; porphyroskelic insepic, with common volcanic shards and rock fragments	−11 cm, AB, fine grained sandstone, light yellowish brown (2.5Y6/3); root traces and burrow as above −30 cm, Bk, calcareous nodules, gray (5Y5/1), up to 15 cm diameter, outermost 1 mm weathering rind of pale yellow (2.5Y7/3), then a 2 mm rind of olive brown (2.5Y4/3), then a 2 mm rind of dark gray (5Y4/1) ; moderately calcareous; agglomeroplasmic calciasepic	−45 cm (A horizon of type Plas paleosol) clayey fine-grained sandstone, pale yellow (2.5Y7/3), non-calcareous; grains of white (2.5Y8/1) and olive gray (5Y4/2); abundant fine (1–2 mm) root traces of light olive brown (2.5Y3/3); insepic agglomeroplasmic microfabric, with common volcanic rock fragments and few shards
Type Tima clay	314.0 m	0 cm, A, clayey fine-grained sandstone, pale brown (10YR6/3), with common drab-haloed root traces, up to 4 cm diameter of white (5Y8/1) and haloes of light gray (5Y7/2); non-calcareous; granular to fine blocky peds; agglomeroplasmic insepic, with rounded and coated granules	−22 cm, Bt, clayey siltstone, yellowish brown (10YR5/4); non-calcareous; granular to fine blocky peds; common drab-haloed root traces as above; agglomeroplasmic insepic microfabric, with rounded and coated granules	−58 cm, C, clayey fine-grained sandstone, light gray (5Y7/2), with granules of pale yellow (5Y8/2) and scattered fine root traces of pale yellow (5Y8/4); non-calcareous: agglomeroplasmic insepic −90 cm, Cy, silcrete, light gray (5Y7/2); non-calcareous; agglomeroplasmic insepic with pockets of banded chalcedony
Type Yapaspa clay	231.0 m	0 cm, A, clayey siltstone, light yellowish brown (2.5Y6/3): granular to fine blocky peds; common fine (1–2 mm) root traces; granular to fine blocky peds; very weakly calcareous	−37 cm, Bk, siltstone, with abundant pale yellow (2.5Y7/3), rounded and scattered calcareous nodules up to 4 cm; moderately calcareous	−45 cm (A horizon of Yapas paleosol on white tuffaceous marker bed), clayey siltstone, grayish brown (2.5Y5/2); granular to fine blocky peds; very weakly calcareous
Type Xaxuspa clay	250 cm (see Retallack et al., 2000, Fig. 117)	0 cm, A, siltstone, grayish green (5G5/2), weakly calcareous with strongly calcareous rhizoconcretions from overlying tabular micritic agglomeroplasmic crystic layer; non-calcareous matrix micofabric intertextic skelmosepic common volcanic shards and rock fragments	−36 cm, Bk, greenish gray (5GY6/1), with common 5–6 cm diameter calcareous nodules white (5Y8/2) with agglomeroplasmic calciasepic and crystic microfabric	−86 cm, C, siltstone, greenish gray (5GY6/1), weakly calcareous; microfabric agglomeroplasmic skelmosepic with common volcanic shards and rock fragments

separated as newly defined pedotypes Xaxuspa, Yapaspa and Plaspa, using a Sahaptin postposition for "in" or "at" (Sapir, 1911; Rigsby, 1965). These shallow calcic paleosols represent different soils and environments from otherwise similar paleosols with deep calcic horizons.

Taxonomic units in contrast are part of a comprehensive classification of the US Soil Conservation Service (Soil Survey Staff, 1999), which require specific laboratory analyses, and are thus interpretive for paleosols altered during burial (Retallack, 1993, 1997b). Proxy chemical and petrographic data are needed to classify paleosols within this and other soil classifications, such as that of the Food and Agriculture Organization of UNESCO (FAO, 1974, 1975a,b) and of the Australian Commonwealth Industrial and Scientific Organization (Stace et al., 1968). One soil classification does not require extensive interpretation of proxies for paleosols, and this coded key of Northcote (1974) has also been applied to the paleosols

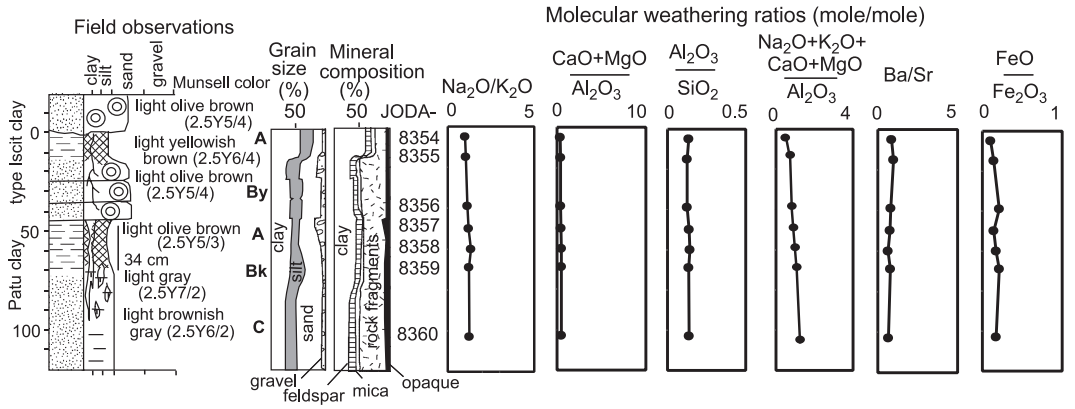

Fig. 12. Detailed section of Iscit and Patu paleosols at 613.8–615.2 m in Bone Creek (Fig. 5). Molecular weathering ratios were chosen as proxies of (from left to right), salinization, calcification, lessivage, base leaching, chemical leaching and gleization (following Retallack, 1997b). Lithological key and other conventions are as for Fig. 3.

(Table 1). Like the paleosol classification of Mack et al. (1993), the Northcote (1974) key does not yet lead to useful paleosol interpretation, compared with better known soil classifications.

3.2. Interpreted paleosol classification

Field pedotypes and their interpreted classification within modern schemes designed for soils are shown in Table 1. Newly proposed pedotypes are described in Table 2, and Table 3 outlines the interpreted paleoenvironmnetal significance of each pedotype and its fossils.

Many of the paleosols are dominated by volcanic shards and probably also had non-crystalline colloids now recrystallized to clinoptolilite and celadonite (Retallack et al., 2000), as in Andisols (suffix "-and" of Soil Survey Staff, 1999) and Andosols (FAO, 1974). Other paleosols have crumb structure, fine root traces and thickness of crumb structure (at

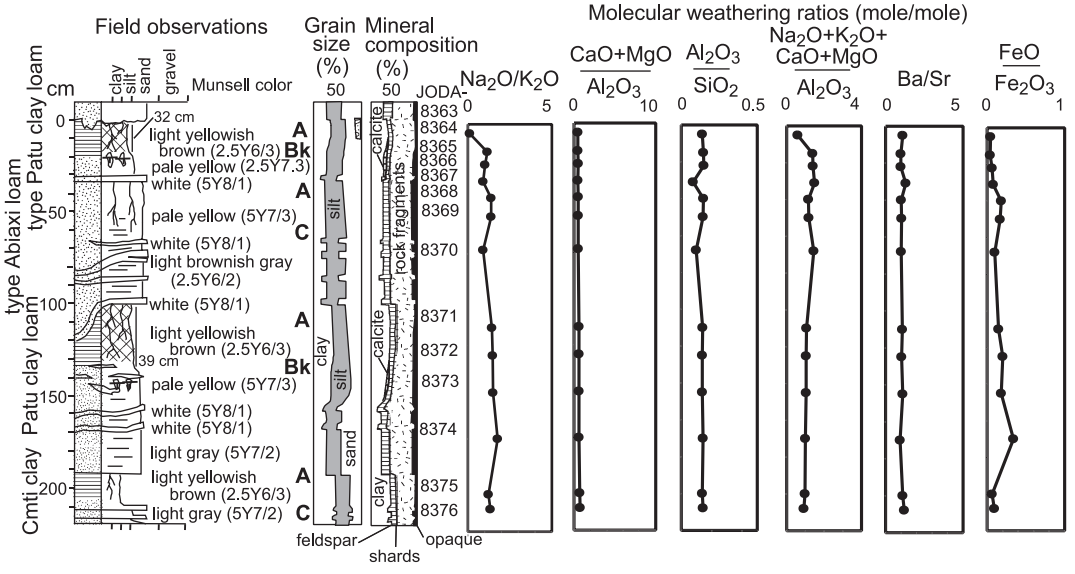

Fig. 13. Detailed section of Patu, Abiaxi and Cmti paleosols at 605.2–607.3 m in Bone Creek (Fig. 5). Conventions are as for Fig. 12.

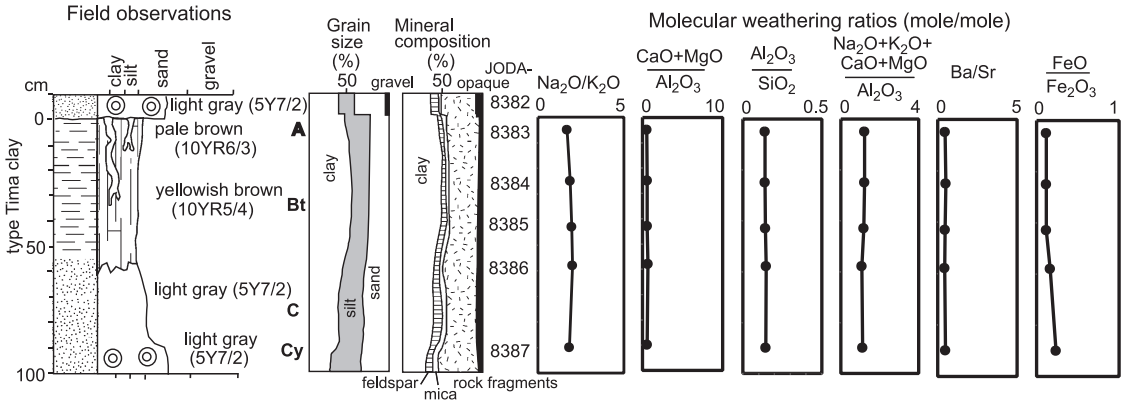

Fig. 14. Detailed section of Tima paleosol at 608.0–609.1 m in Bone Creek (Fig. 5). Conventions are as for Fig. 12.

least 25 cm) to qualify as Mollisols (suffix "-oll" of Soil Survey Staff, 1999) and Kastanozems (of FAO, 1974). Other paleosols have high soda–potash ratios, shallow nodules and concretions of calcite and chalcedony indicative of Aridisols (suffix "-id" of Soil Survey Staff, 1999) and of Xerosols, Solonchak and Solonetz (of FAO, 1974). Other paleosols are weakly developed with bedding planes of sedimentary parent material little disrupted by root traces as in Entisols (suffix "-ent" of Soil Survey Staff, 1999) and Fluvisols (FAO, 1974).

3.3. Paleoenvironmental implications of classification

A general concept of paleoenvironment can be gained from taxonomic considerations, accepting the identifications given in Table 1 and their supporting proxies discussed above. For example, some of the paleosols (Xaxus, Yapas, Micay) in the Turtle Cove and lower Haystack Valley Members are taxonomically similar to the suite of soils now found near Tehuacán, Mexico (map unit To2-2bc of FAO, 1975b). This intermontane basin within the central Transmexican Volcanic Belt includes grassy deciduous woodlands and bunch grassland (Retallack et al., 2000). In contrast, other paleosols in the Turtle Cove and lower Haystack Valley Members (Xaxuspa and Yapaspa) are more like desert soils of the basins north of Mexico City to Cerritos (map unit Xk7-2a of FAO, 1975b). These grassy woodland and desert shrubland paleosols alternate through much of the Turtle Cove and lower Haystack Valley Members, and comparable alternation of white silty paleosols (Plas and Plaspa) continues within the Kimberly Member.

Modern soilscapes taxonomically comparable with Plas paleosols of the Kimberly and middle Haystack

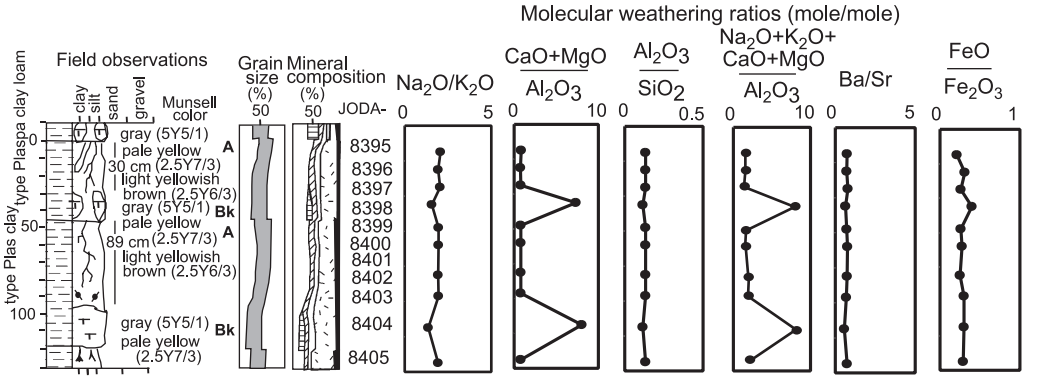

Fig. 15. Detailed section of Plaspa and Plas paleosols at 274.6–276.0 m in Bone Creek (Fig. 5). Conventions are as for Fig. 12.

Table 3
Interpreted paleoenvironment of paleosols of the upper John Day Formation

Pedotype	Paleoclimate	Former vegetation	Former animals	Paleotopography	Parent materials	Time for formation
Abiaxi	Insufficiently developed as an indicator	Saline scrub	None found	Salt pans	Rhyodacitic volcaniclastic sand	0.01–0.1 ka
Cmti	Insufficiently developed as an indicator	Early successional riparian grassland	Horse (*Parahippus*), camel (*G. sternbergi*), chalicothere (*Moropus oregonensis*), bear–dog (*Daphaenodon*)	Dry silty swales in river channels	Redeposited rhyodacitic silts and sands	0.005–0.01 ka
Micay	Insufficiently developed as an indicator	Early successional riparian vegetation	None found	River banks and point bars	Tuffaceous fluvially redeposited silts and sands	0.005–0.01 ka
Iscit	Semiarid seasonally dry	Grassy woodland	None found	Floodplain	Vitric-tuffaceous siltstone	1–5 ka
Patu	Semiarid (300–400 mm mean annual precipitation) seasonally dry	Lightly wooded short sod grassland	None found	Floodplain	Tuffaceous siltstone	0.5–2 ka
Plas	Semiarid (400–500 mm mean annual precipitation)	Sagebrush shrubland	Horse (*Miohippus*)	Floodplain	Tuffaceous silts	2–7 ka
Plaspa	Semiarid (300–400 mm mean annual precipitation)	Desert scrub	Pocket gopher (*E. planifrons*), mouse deer (*H. minutus*)	Floodplain	Tuffaceous silts	2–7 ka
Tima	Semiarid, seasonally dry	Dry woodland	None found	Floodplain	Vitric tuffaceous siltstone	2–7 ka
Yapas	Subhumid (600–1050 mm mean annual precipitation) seasonally dry	Open grassy woodland and wooded grassland	None found in this study (but see Retallack et al., 2000)	Well-drained low relief floodplain	Redeposited rhyo-dacitic tuff	10–50 ka
Yapaspa	Semiarid (350–600 mm mean annual precipitation)	Sagebrush shrubland	None found	Well-drained low relief floodplain	Redeposited rhyodacitic crystal tuff	10–50 ka
Xaxus	Subhumid–semiarid (500–850 mm mean annual precipitation) seasonally wet	Lightly wooded, seasonally wet meadow	Earthworms (*Edaphichium*), dung beetles (*Pallichnus*), termites (*Termitichnus*), snails (*Vespericola dalli, Monadenia marginicola*), pocket gophers (*Entoptychus* spp), mouse deer (*Nanotragulus planiceps*), oreodonts (*Merycochoerus superbus*, *Eporeodon occidentalis*, *Merychyus arenarum*), rhinos (*Diceratherium* sp.), horses (*Miohippus–Mesohippus* spp.)	Seasonally wet alluvial lowland	Redeposied rhyodacitic tuff	10–50 ka
Xaxuspa	Semiarid (300–500 mm mean annual precipitation)	Sagebrush desert grassland	Cicadas (*Taenidium*), snails ("*Polygrya*" *expansa*, *Monadenia dubiosa*), pocket gophers (*Entoptychus* spp.) mouse deer (*H. hesperius*)	Seasonally wet alluvial lowland	Redeposited rhyodacitic tuff	10–50 ka

Valley Members are in the western Chihuahua Desert of the Central Mexican Plateau from Moctezuma north to Cuidad Camargo (map unit Xk6-2ab of FAO, 1975b), but Plaspa paleosols are more like soilscapes further north in Chihuahua near Salinal (map unitYk9-2ab of FAO, 1975b). The desert shrublands to the south have common yucca and saltbush, but those to the north are sparser, and both lack the large saguaro cactus that characterizes Sonoran desert vegetation.

Paleosols of the upper Haystack Valley Member in Johnson and Bone Creeks do not show repetitious alternations, and resemble soils around Great Salt Lake, Utah (map unit So1-3a of FAO, 1975a). This is an intermontane basin of saltbush scrub and sagebrush steppe, with local riparian woodland of cottonwood and willow.

4. Paleoenvironment interpreted from soil features

4.1. Paleoclimate

Two separate soil features can be used to infer former mean annual precipitation from paleosols, depth to carbonate and chemical composition. The depth to carbonate (D, in cm) in paleosols is related to precipitation (P, in mm) by the following equation (Retallack, 1994b, 2000; Royer, 1999; Wynn and Retallack, 2001):

$$P = 139.6 + 6.388D - 0.01303D^2$$

The paleosols measured had carbonate nodules or carbonate-rich concretions (not wisps or thick continuous layers) and were developed on unconsolidated loess and alluvium (not bedrock) of an alluvial bottomland (not hill slopes). These variables unconstrained would compromise the relationship between depth to carbonate and precipitation (Royer, 1999; Retallack, 2000). No correction was made for erosion of paleosols because root traces and paleosol surfaces did not appear disrupted, and because rates of sediment accumulation were unusually high (Fig. 9; Retallack, 1998). No correction was made for atmospheric CO_2 levels either, because these have not been shown to have been high or variable during the late Oligocene or early Miocene (Retallack, 2002b). The depth to carbonate was corrected for burial compaction (using Inceptisol physical constants of Sheldon and Retallack, 2001).

A second estimate of mean annual precipitation (P, in mm) came from chemical index of alteration without potassium (C, which is the molar ratio of alumina over alumina plus soda, lime and magnesia times 100) of paleosol subsurface (Bt or Bw) horizons (Sheldon et al., 2002):

$$P = 221.12e^{0.0197C}$$

This estimate (open boxes in Fig. 16) did not seem as sensitive to short episodes of desertification as the depth to carbonate (black circles in Fig. 16) for three reasons. First, degree of chemical weathering would have been negligible and erosion of upland soils more widespread during episodes of desertification (Bestland, 2000). Second, this transfer function is calibrated for precipitation between 200 and 1600 per annum, and not for higher or lower precipitation (Sheldon et al., 2002). Third, the expense of chemical analysis did not permit as many determinations as were made of depth to carbonate. Nevertheless, both transfer functions are in substantial agreement in indicating semiarid to arid conditions until about 19 Ma, then a subsequent swing toward subhumid conditions.

Depth to carbonate and recurrent silty, loessial facies indicate drier intervals at 25.8, 23.2, 21.1 and 19.2 Ma (Fig. 16). These times of aridity were global, because coeval arid phases are seen in the North American Great Plains (26 Ma Monroe Creek Formation, 23 Ma Rosebud Formation, 21 Ma Harrison Formation and 19 Ma Anderson Ranch Formation: Retallack, 1997a; Hunt, 2002), and also in deep-sea cores, where arid phases correspond to glacial advances in Antarctica (Oi2 at 25 Ma and Mi1 at 23 Ma of Zachos et al., 2001a,b). The terminal Oligocene aridification is striking in outcrop, and the caliche caprock north of Kimberly, is very similar to the terminal Monroe Creek Formation caprock in Smiley Canyon and elsewhere in Nebraska (Schultz and Stout, 1981).

A remarkable feature of the paleoprecipitation record from depth to carbonate (Fig. 16) is high variability on Milankovitch temporal scales (10^3–10^5 years), as has been noted before in the John Day Formation (Bestland and Swisher, 1996). Each

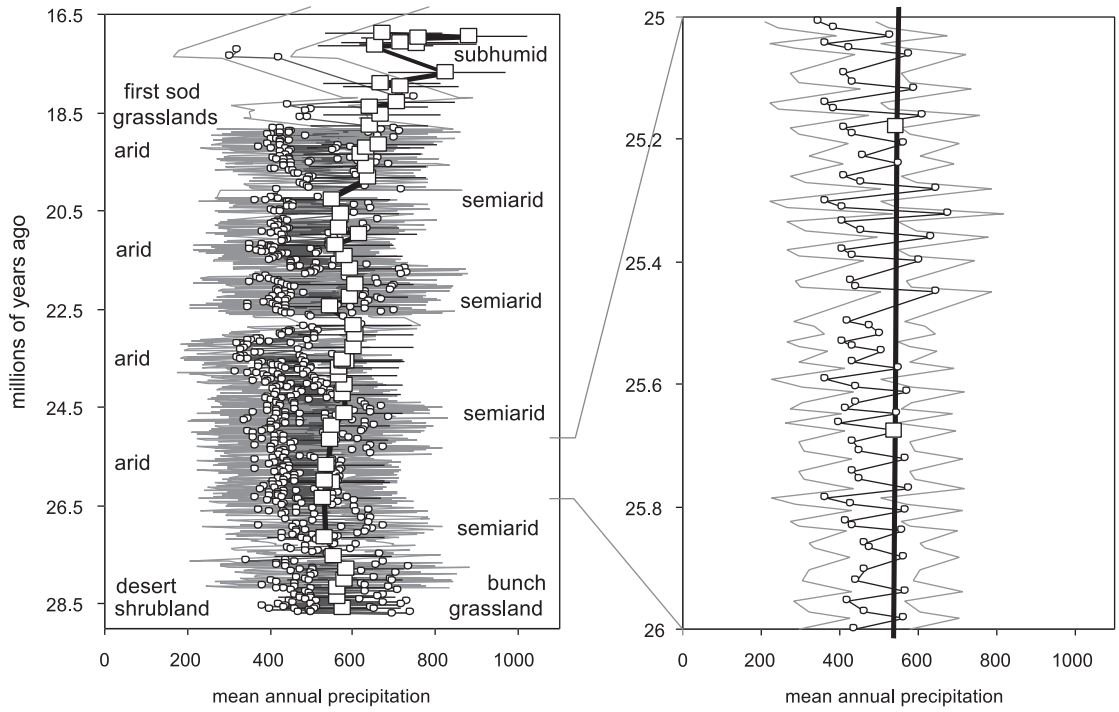

Fig. 16. Milankovitch scale (41–100 ka) fluctuation (B, right, in portion of record) and broader trends of paleoprecipitation (A, left, for whole record) inferred from depth to Bk horizons (open circles) and from chemical composition of Bt horizons (open squares) in the upper John Day Formation near Kimberly and Spray. Chemical data are mainly for deep carbonate (more humid) paleosols of triplets like those of Fig. 17. Error envelopes and bars (thin gray lines) are one standard error. Only the interval 28.5–23.5 is well dated radiometrically, with the younger part extrapolated using biostratigraphic tie points (Fig. 9).

cycle consists of three paleosols (Fig. 17), in a pattern that is repeated throughout the upper John Day Formation (Figs. 3–8) with the exception of the uppermost parts of the Johnson Canyon and Bone Creek sections (Figs. 5 and 8). The basal Xaxus paleosol of each cycle has a deep (>50 cm) calcic horizon, that is usually thick (15–30 cm), tabular and restricted to a limited thickness of about 30 cm. This paleosol is then capped by two Xaxuspa paleosols with shallow (<50 cm) calcic horizons, that have abundant small, rounded nodules (2–15 cm) scattered through a substantial thickness (50 cm) of rock (Fig. 17). Yapas and Yapaspa pedotypes show similar alternation, as do Plas and Plaspa pedotypes, but these latter oscillate around 45 cm rather than 50 cm, and have smaller nodules, perhaps reflecting a shorter time for formation. These triplet patterns are similar to the pattern of rapid termination to humid–warm climate, and long descent into dry–cold climate seen in Quaternary paleosols and phytoliths of the Palouse Loess of Washington (Busacca, 1999; Blinnikov et al., 2002). The Milankovitch frequencies observed in Quaternary paleosols are 23, 41 and 100 ka, with either 100 ka or 41 ka dominant. Estimated times for formation of Oligocene triplets of a Xaxus and two Xaxuspa paleosols (Table 3) are consistent with 41–100 ka duration, but Plas–Plaspa triplets may represent shorter intervals of 23–41 ka. The radiometrically dated first 5.1 million years of this sequence (Fig. 9) has 105 Xaxus–Xaxuspa or comparable cycles, again consistent with Milankovitch scale temporal change.

Milankovitch scale variation was not seen in the Hemingfordian beds of Johnson and Bone Creeks, where a paleoclimatic change is indicated by the appearance of sparsely to non-calcareous silica-cemented rhizoconcretions (in Patu pedotype) and horizons (in Tima and Iscit pedotypes). The genesis

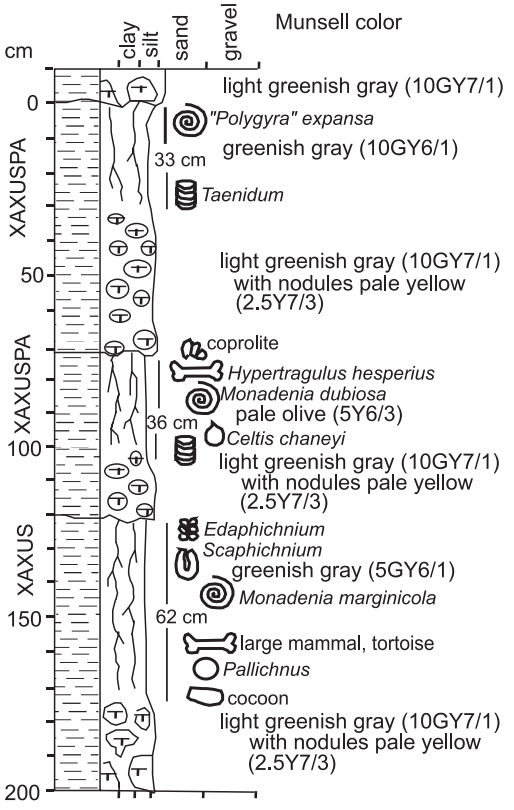

Fig. 17. Detailed section of Xaxus and two Xaxuspa paleosols at Roundup Flat (Fig. 4; 131–134 m above Picture Gorge tuff in composite section). Such triplet patterns of paleosols alternate on Milankovitch time scales.

of such silica-cemented horizons in modern soils has been studied in southeastern Australia (Chartres and Norton, 1993) and southwestern US, where they are called duripans (Chadwick et al., 1987, 1995), in Mexico where they are known as tepetaté (Oleschko, 1990; Flores-Román et al., 1996) and in Ecuador as cangahua (Creutzberg et al., 1990). Extensive duripans form in vitric volcanic tuffs, which release abundant silica during humid weathering (Flores-Román et al., 1996), and from the activity of sulfur-reducing bacteria in organic soils (Birnbaum et al., 1986; Retallack and Alonso-Zarza, 1998). Silicification of plant material also occurs in hot springs (Jones et al., 1998), but the rhizoconcretions of the Hemingfordian beds do not show cellular permineralization found in hot springs. Volcanic origin of silcretes in paleosols of the Hemingfordian beds is unlikely, because they have smaller amounts of volcanic shards than underlying paleosols, as an indication of declining volcanic activity. Furthermore, Hemingfordian paleosols are surprisingly rich in sodium (soda–potash ratios more than 1: Figs. 12–14), indicating salinization in a paleoclimate much drier than Mexican and Ecuadorian high-altitude volcanic soils with silica-cemented layers. The scattered silica is most like opal and chalcedony of dry and highly seasonal soils in which highly alkaline groundwater increases silica dissolution and remobilization (Chadwick et al., 1987, 1995). Banding in the upper John Day Formation silcretes (Fig. 18C,D) is evidence of strong climatic seasonality, probably wet–dry seasonality in an overall semiarid paleoclimatic regime.

Silica-enriched paleosols of the Hemingfordian beds (Figs. 5 and 8) are in striking contrast to the carbonate-nodule-studded Xaxus, Plas and Yapas paleosols of the rest of the John Day Formation (Figs. 3–8). In North America today, calcareous nodules are most abundant in the summer-wet interior deserts of the Great Plains, Texas, New Mexico and north-central Mexico (Gile et al., 1981), whereas duripans and lesser carbonate are found in the deserts of summer-dry California, Nevada and Oregon (Chadwick et al., 1987, 1995). This distinctive silica-encrusted paleosol suite may represent the onset of current summer-dry (Mediterranean) climate in Oregon at around 19 Ma (Fig. 9), and perhaps its current extent from California north to central Washington and east as far as Utah (FAO, 1975a). An increase in both aridity and seasonality at about this time is also indicated by oxygen isotopic composition of equid teeth in central Oregon (Kohn et al., 2002).

4.2. Paleoflora

The only fossil plants seen in paleosols near Kimberly and Spray were hackberry endocarps (Chaney, 1925), but these were only abundant in the lower part of the Johnson Creek section (Fig. 8). Hackberry endocarps are a biased fossil record because of their biomineralization, which is unusual for plants (Retallack, 1998). Fossil root traces and rhizoconcretions of the upper John Day Formation include both stout, tapering forms and fine filaments, interpreted as roots of a mix of grasses and trees. Calcareous nodules and

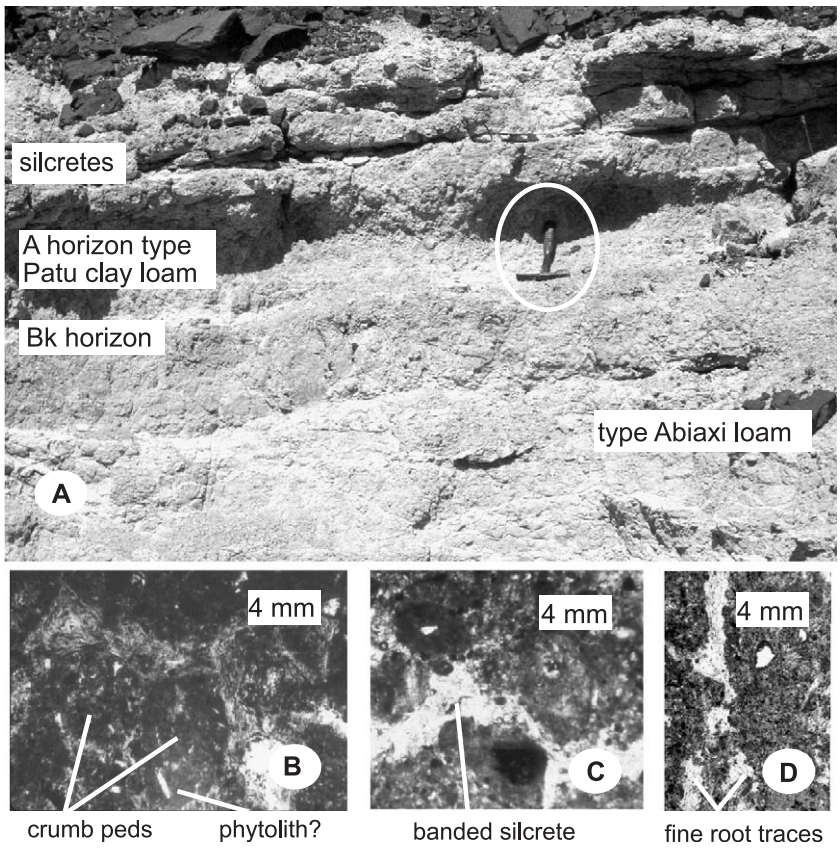

Fig. 18. (A) Crumb structure in type Patu clay loam pedotype (607 m above Picture Gorge tuff), interpreted as evidence for sod grasslands, and overlying banded silcrete, interpreted as evidence for strong paleoclimatic seasonality in an arid regime (hammer in ellipse for scale); (B–D) photomicrographs under crossed nicols of (B) crumb ped from type Patu clay loam (JODA8365), (C) banded silica cement from silcrete below Iscit paleosol at 605 m (JODA8355); (D) silica-replaced fine root trace from type Patu clay loam (JODA8367).

high soda content are also evidence of open, dry vegetation. Plausible modern analogs are bunch grasslands and grassy deciduous forests of the Central Transmexican Volcanic Belt near Tehuacán (Retallack et al., 2000).

Janis (2000) has suggested that Oligocene vegetation in the Great Plains and western North America may have been comparable to South African fynbos, which is a small-leaved shrubland of nutrient-poor sandy soils on early Paleozoic quartzites of the Cape Mountains (Pauw and Johnson, 1999). Fynbos is also comparable to the heath and shrubland of the Hawkesbury Sandstone around Sydney, Australia (Beadle, 1981). Oligocene–Miocene volcanic soils were a different and more fertile substrate (Retallack, 1983; Retallack et al., 2000). Fynbos, heath and shrublands have common sedges, but few, if any, grasses or earthworms. In contrast, Oligocene–Miocene paleosols have grass-like root traces, earthworm trace fossils, granular-crumb ped structure, hackberry pits (Retallack, 1983; Retallack et al., 2000) and silica phytoliths of grasses (Strömberg, 2002, this volume). Furthermore, fynbos has small, sclerophyll, evergreen leaves, unlike the hackberry (*Celtis*) known from Oligocene–Miocene paleosols in Oregon and South Dakota (Chaney, 1925). Oligocene fossil floras of western North America have revealed a variety of plant communities (Wing, 1987, 1998), but nothing as small-leaved or scleromorphic as fynbos.

Another clue to vegetation of the past comes from distinctive assemblages of trace fossils, which are

remarkably similar to trace fossil assemblages of the Quaternary Palouse Loess of Washington state (Tate, 1998; O'Geen and Busacca, 2001). The shallow-calcic (< 50 cm to Bk), green (Xaxuspa) paleosols have abundant backfilled burrows of the ichnogenus *Taenidium* (Fig. 19F), which were never seen in deep-calcic (>50 cm to Bk) Xaxus or other deep-calcic pedotypes. The deep-calcic Xaxus paleosols in contrast have trace fossils of *Edaphichnium* and *Pallichnus* (Fig. 19A–E). This striking alternation of trace fossil assemblages is found throughout the stratigraphic range of these trace fossils (Figs. 3–8, 10). Modern *Taenidium* in comparable soils and paleosols of the Palouse region of Washington is constructed by cicada species (*Okanaga vanduziae*), which are restricted to sagebrush desert vegetation and which vanish at the ecotone with grassland (O'Geen and Busacca, 2001). In contrast, *Edaphichnium* is the chimney of earthworms (Bown, 1982; Bown and Kraus, 1983) and such pelletoidal fabric is diagnostic of grassland soils and paleosols in Quaternary loess of eastern Washington (Tate, 1998). *Pallichnus* is an ichnogenus of dung beetle boli (Retallack, 1984), and part of the *Coprinisphaera* ichnofacies, also characteristic of grassland soils and paleosols (Retallack, 1990; Genise et al., 2000). Also from a Xaxus paleosol is *Termitichnus*, nests of ground-dwelling termites (Smith et al., 1993), but the Oregon nests are not elaborate and are found at only one stratigraphic level (Fig. 10). In summary, the trace fossil assemblages indicate alternation between sagebrush desert and short desert grassland (Fig. 17), and local age calibration (Fig. 9) shows that this alternation was on Milankovitch temporal frequencies.

This alternation of shrubland and desert grassland changed by 24 Ma during deposition of the upper John Day Formation to alternation of desert shrubland and desert scrub. Trace fossils become rare and are mainly small mammal burrows within the Kimberly Member, which is silty and loessic. Plas and Plaspa aleosols in this eolianite facies have shallow calcic horizons, and weakly pedal soil structure, with little trace of filamentous root traces like those of grasses (Fig. 15). The Kimberly Member also has a white to pink hue different from other parts of the John Day Formation.

The lower Haystack Valley Member in Balm Creek has a suite of green (Xaxus and Xaxuspa) and brown (Yapas and Yapaspa) paleosols like those of the upper Turtle Cove Member, although darker, more indurated and less calcareous. This paleosol suite indicates a more humid, though still semiarid climate, and reversion of vegetation to wooded grassland and desert shrubland. In the middle Haystack Member of Balm Creek, Black Bone Hill and Johnson Creek sections, the eolianite facies with pale paleosols (Plas and Plaspa) indicates later climatic drying and reappearance of desert scrub.

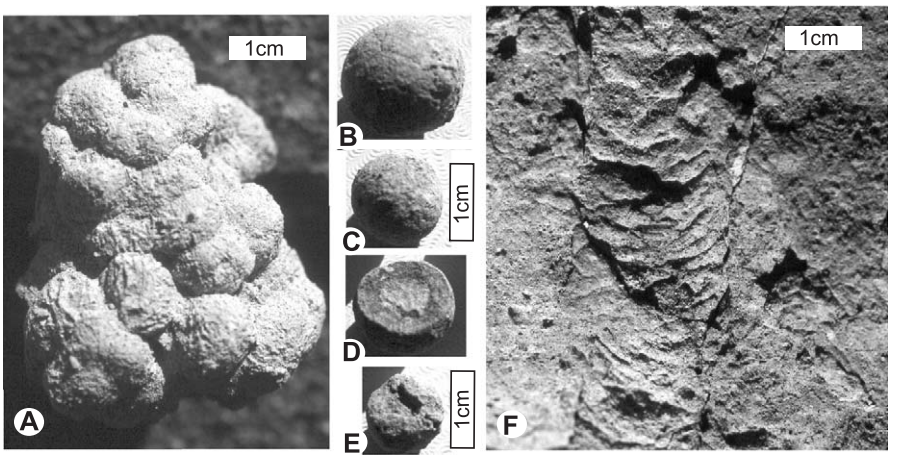

Fig. 19. Trace fossils of *Edaphichnium* (A), *Pallichnus* (B–E) and *Taenidium* (F) from the Oligocene Turtle Cove Member of the John Day Formation. Localities–specimen numbers are (A) Sorefoot Creek–JODA8343, (B–E) Roundup Flat, 188.6 m level–JODA8177, and (F) Roundup Flat 207.4 m level–JODA8206. All traces are to the same scale.

Hemingfordian beds of Bone and Johnson Creeks include a distinctive new suite of paleosols (Figs. 5, 8, 11–14) and distinctive new soil structures (Fig. 18A–D). Some of these paleosols (Iscit and Patu pedotypes in Johnson Creek) are the oldest (at 19 Ma) currently known in Oregon with pervasive crumb peds and fine networks of mainly filamentous root traces. Such finely crumb-structured paleosols are the same geological age in the Great Plains of North America (19 Ma in Anderson Ranch Formation; Retallack, 1997a; MacFadden and Hunt, 1998; Hunt, 2002). Crumb structure is found in modern sod grasslands, which have such a dense root mat that they can be excavated and rolled up like a carpet for replanting (Retallack, 2001a). This soil structure differs from the fine, subangular, blocky structure and scattered fine root traces of presumed bunch grasses in geologically older paleosols in the John Day Formation (Retallack et al., 2000), and the North American Great Plains (Retallack, 1983). Considering also the shallow carbonate and silica of associated paleosols, this early sod formed under short grassland as part of a vegetative mosaic including dry woodlands.

The suggested transition from Oligocene bunch grasslands to Miocene sod grasslands probably involved new species of grasses, because of the very different climatic regime indicated by paleosols in Oregon. At present, the summer-dry western grasslands of California, Oregon, Washington, Idaho and Utah are within the western wheat grass (*Agropyron spicatum*) province, whereas dry parts of the summer-wet Great Plains and the northern Mexican Plateau are within the buffalo grass (*Bouteloua gracilis*) province (Leopold and Denton, 1987). The actual species of grasses involved during the Miocene and Oligocene are unknown, although such western steppe taxa as sagebrush (*Artemisia*), greasewood (*Sarcobatus*) and mormon tea (*Ephedra*) are evident from pollen records in the western US well back into the Eocene (Leopold et al., 1992), and Miocene spread of open-habitat pooids, arundinoids and panicoids in the Great Plains is inferred from phytoliths (Strömberg, this volume). Hemingfordian mammals of Oregon and the Great Plains are largely different species, but these faunas share many genera (Rensberger, 1973, 1983; Dingus, 1990; Woodburne and Robinson, 1977; Coombs et al., 2001).

4.3. Paleofauna

In addition to insect and earthworm trace fossils characteristic of particular plant communities, fossil mammal bone, turtle scute and snail shell are common within the upper John Day Formation, especially within large (>20 cm diameter) paleosol nodules in a form of preservation very similar to that documented by Downing and Park (1998). Mammalian faunas changed considerably with changes in paleoclimate and vegetation during the late Oligocene and early Miocene (Fig. 10), which was a period of marked modernization in ungulates (Janis, 2000) and grass phytoliths (Strömberg, this volume). Oreodont-dominated faunas persisted throughout the Turtle Cove Member, for which limited spatial and temporal variation of habitat is indicated by dominance of green Xaxus and Xaxuspa paleosols (Figs. 3 and 4). The gracile oreodont *Eporeodon occidentalis*, three-toed horses (*Mesohippus* spp., *Miohippus* spp.) and rhinos (*Diceratherium* spp.) are common throughout the lower and middle Turtle Cove Member (Fremd, 1988, 1991, 1993; Fremd et al., 1994). The rhinos are hypsodont and so presumed grazers, but the horses are not hypsodont. Nevertheless, microwear studies indicate substantial amounts of abrasive grass in Oligocene horse diets (Solounias and Semprebon, 2002). There also are common fossil tortoises (Hay, 1908), and a diverse assemblage of fossil land snails (Hanna, 1920, 1922; Pilsbry, 1939–48; Roth, 1986; Pierce, 1992).

Climatic change to arid conditions with muted variation at about 25.8 Ma (Fig. 16) coincides with the first appearance of hoglike oreodonts (*Merycoochoerus superbus*; Lander, 1998) and of pocket gophers (*Entoptychus* spp.; Rensberger, 1971). This also is the beginning of the "cat gap" (Van Valkenburgh, 1991) and "entelodont gap" (Foss and Fremd, 2001), a period of some 7 million years when there were no nimravids, felids, or entelodonts in North America. These taxa re-entered North America, probably from Europe, during the Hemingfordian (18.8 Ma according to MacFadden and Hunt, 1998). Faunal overturn at 25.8 Ma is the basis for division of the Arikareean NALMA into "Monroecreekian", then "Harrisonian" (Alroy, 2000).

Fossils remain common in green calcareous (Xaxus and Xaxuspa) paleosols after this faunal overturn at

about 25.8 Ma. When the last of these green paleosols, dated at about 24.5 Ma (Fig. 5), is covered by a sequence of pinkish-white calcareous (Plas and Plaspa) paleosols of drier inferred paleoclimate of the Kimberly Member, bones become rare (Fig. 16). *Merycochoerus*, *Miohippus* and *Diceratherium* persist, but the common mouse deer species *Hypertragulus hesperius* is replaced by a smaller species *Hypertragulus minutus* (Webb, 1998). Pocket gophers (*E. planifrons* and *E. individens*) evolved to larger size, greater hypsodonty and more marked fossorial adaptations (Korth, 1994), and fossil rodent burrows are common in the paleosols. Many of the rodent burrows are nuclei of carbonate nodules, which are gray with organic matter and manganese, as if encrusted with roots and algae, like comparable burrows in the Harrison Formation of Nebraska (Retallack, 1990). In contrast, Xaxus paleosol nodules and nodularized burrows have less carbon than their matrix, and their orange micrite contrasts with the gray-green clayey matrix. No large tortoises or snails were found in the Kimberly Member, perhaps because of desertification indicated by the shallow depth to carbonate in the paleosols (Fig. 16).

Return of more humid and grassy vegetation inferred from green (Xaxus and Xaxuspa) and brown (Yapas and Yapaspa) paleosols in the early Miocene lower Haystack Member of Balm Creek is within the youngest of the entoptychine zones (*E. individens*: Rensberger, 1971), where there is a new fauna of oreodons (*Merychyus arenarum*), and camels (“*Paratylopus*” *cameloides*: Fremd et al., 1994).

Within Hemingfordian beds with aridland paleosols (Plas and Plaspa) of Black Bone Hill, Johnson and Bone Creeks, the mammal fauna is again changed (Coombs, 1978; Fremd et al., 1994; Lander, 1998; MacFadden, 1998; Webb, 1998; Coombs et al., 2001). The fauna now has very different rodents (*Mylagaulodon*, *Schizodontomys*) and is dominated by hypsodont horses (*Parahippus*) and camels (*Gentilicamelus*, “*Paratylopus*”), rather than oreodonts (Fig. 10). This is the beginning of the Miocene grazing guild of wooded grasslands, which reached its greatest diversity by about 10–15 Ma (Webb, 1998; Janis et al., 2002). Unfortunately, fossils are known mainly from paleochannels, rather than from paleosols (Coombs et al., 2001), but the appearance of sod grassland paleosols (Iscit and Patu) is compatible with the mammalian ecological shift toward grazing.

4.4. Paleotopography

Paleocurrents (Fig. 11) and paleosol distribution are evidence of a broad northwest-flowing river basin during deposition of the upper John Day Formation. The wide extent of this alluvial lowland is revealed by muted lateral thickness variation of volcanic ashes within the Turtle Cove Formation. The current location of Longview Ranch was near the eastern margin of the seasonally inundated floodplain, represented by green unoxidized (Xaxus) paleosols. Evidence for this comes from observations 5 km to the northeast in Rudio Canyon at the same stratigraphic interval of ash-flow tuff *H*, where there is a sequence of red, clayey (Luca) paleosols of well-drained interfluves (Retallack et al., 2000). The paleoslope 100 km to the west into the current area of the Painted Hills was more gentle, because only a few green, poorly drained (Xaxus) paleosols are found there, along with brown, lowland, moderately drained (Maqas and Yapas) paleosols (Retallack et al., 2000). To the west were eroded hills of a moribund volcanic arc, which was active in Eocene time. This whole region was an Oligocene and Miocene back-arc basin to the ancestral Cascades volcanic arc (Retallack et al., 2000).

Considerable local topography was generated by paleovalleys preserved within the Haystack Valley Member. These erosional episodes do not appear to be related to tectonic uplift, local doming or faulting, because they are concordant with successive thick flows of the Columbia River Basalt Group (Fisher and Rensberger, 1972). Local doming and faulting postdated these flood basalts, and was coeval with middle Miocene accumulation of the Mascall Formation, as can be seen from sedimentary onlap of that formation south of Picture Gorge (Retallack et al., 2002). Valley-cutting events at 23.2, 21.1 and 19.2 Ma were the culmination of climatic cooling and drying trends, as revealed by declining depth to carbonate in paleosols (Fig. 16). The Hemingfordian beds of Bone Creek also show an upward drying cycle, terminating with a thick duripan (618 m in Fig. 5) probably about 17 Ma in age (Fig. 9).

4.5. Paleosol parent materials

Paleosols of the upper John Day Formation formed largely on redeposited rhyodacitic volcanic ash, which varies little in chemical or mineral composition (Retallack et al., 2002). Volcanic shards are common, and chemical analyses indicate that the paleosols were little altered from their parent material (Bestland, 2000). Some of the paleosols formed directly on fresh volcanic airfall ash, which remains as the Deep Creek, Biotite, Tin Roof and ATR tuffs (Fig. 8). Most paleosols were formed on ash that fell elsewhere, weathered to some extent, then mixed and redeposited by wind and water. Rock fragments include mainly rhyodacite, but also rare basalt, schist and granite. Volcanic shards are rare, and rock fragments much more common in the Hemingfordian beds than in the rest of the John Day Formation, perhaps due to deposition in valleys eroded into the underlying rocks and to declining rate of tuffaceous volcanism.

5. Discussion

Late Oligocene and early Miocene was a time of profound fluctuation in paleoclimate, when the Antarctic ice cap was established and expanded for the first time to near sea level (Zachos et al., 2001a). It was also a time of evolutionary radiation for plants (Jacobs et al., 1999) and mammals of grasslands (MacFadden, 2000). The Upper John Day Formation paleosol sequence is a high-resolution record of these climatic and biotic events (Table 3; Figs. 20 and 21).

5.1. Oligo–Miocene climatic events

Paleosols of the upper John Day Formation exposed on Longview Ranch are a paleoclimatic archive that in places is superior to that of deep-sea cores. The most complete deep sea record of late Oligocene climate record from the oxygen isotopic composition of foraminifera had to be spliced together from several cores because of core recovery problems, then tuned to orbital cyclicity and still some climatic beats are missing (Zachos et al., 2001b). The upper Turtle Cove and lower Kimberly Members of the John Day Formation, however, are unlikely to be missing a single 100 ka beat in an untuned record of 105 paleoclimatic cycles within the 5.1 million year duration of these rocks (Figs. 3–5). The upper Kimberly and Haystack Valley Members appear comparably complete within their measured sections (Figs. 6–8), but less securely dated, and there may be disconformities between measured sections. These rocks crop out in extensive large badlands with ample lateral exposure of each paleoclimatic cycle. Large amplitude cycles in oxygen isotopic composition of marine foraminifera (Zachos et al., 2001a) are found at the same time as large amplitude cycles in paleosol carbonate depth in Oregon (Fig. 16), and small amplitude cycles are found in both during intervening times. One of these times of low amplitude climatic fluctuation was at the Oligocene–Miocene boundary (23.2 Ma) and the other was within the late Oligocene (25.8 Ma). Both were times of arid climate indicated by paleosols (Fig. 16), and the paleoclimatic shift had profound effects on fossil mammals in central Oregon (Fremd et al., 1994; Hunt and Stepleton, 2001). Both were also times of Antarctic ice expansion, revealed by ice rafted debris in deep sea cores (Zachos et al., 2001a).

An especially profound paleoclimatic change at about 19 Ma is recorded in the Johnson Creek section. Before that time most paleosols had large calcareous nodules, like paleosols common throughout the Cenozoic in the Great Plains of North America. After that time, large carbonate nodules are uncommon, with carbonate limited to partial cementation of chalcedony-encrusted root traces. Hemingfordian paleosols of Bone and Johnson Creeks had natric (soda rich) clays and banded, botryoidal and mammillar silcrete, like that at the top of the Harrison Formation in Nebraska (Retallack, 1997a). Hemingfordian silcretes of Bone and Johnson Creeks are most like those now found in arid Nevada and California (Chadwick et al., 1987, 1995). The Great Plains now has a climate with summer rain fed by monsoon-like circulation of warm air masses from the Gulf of Mexico. The Pacific Northwest, however, has long dry summers because of cool, high-pressure air masses generated by cold ocean currents moving south from Alaska. This is a fundamental difference between climates of the two regions. The Pacific Northwest has a

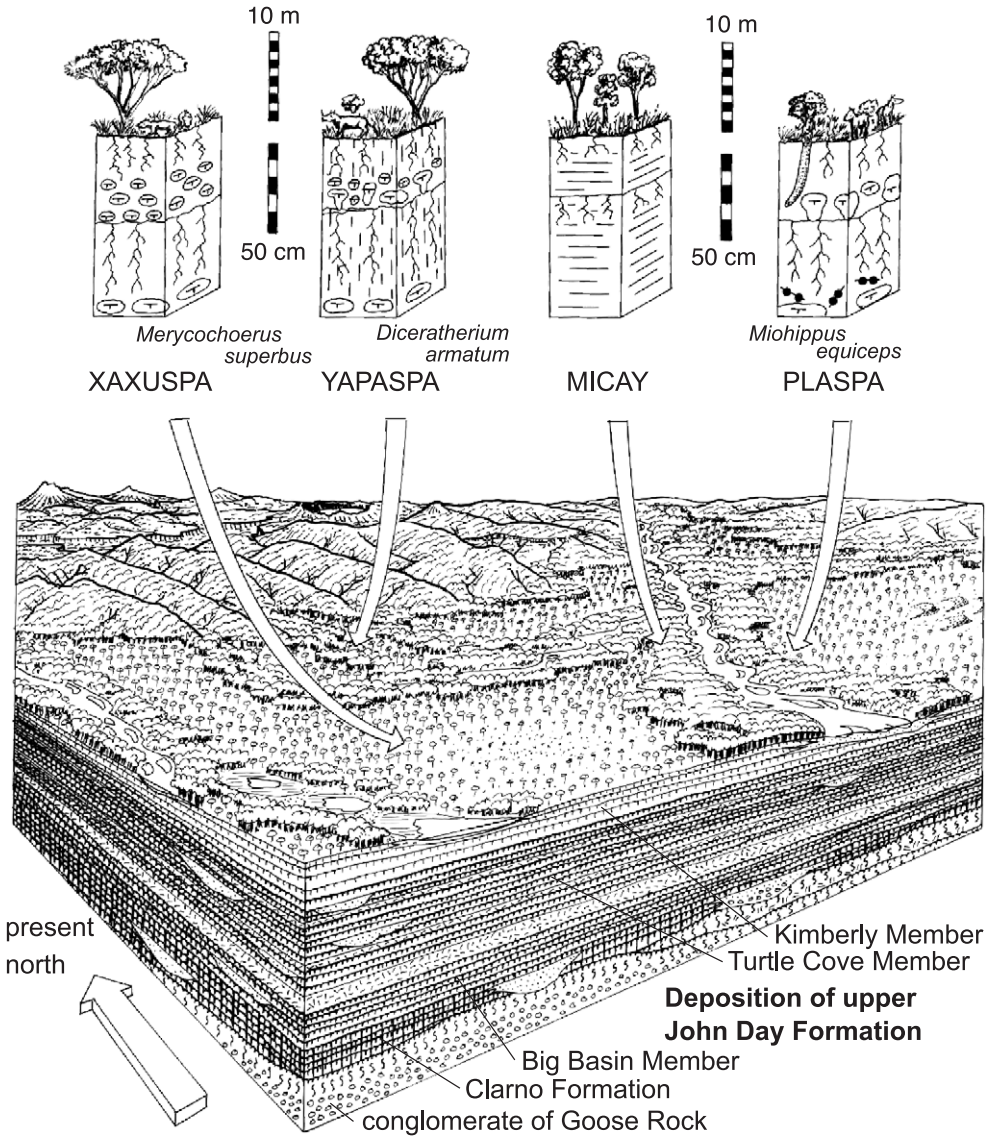

Fig. 20. A reconstruction of Longview Ranch during Late Oligocene (late Arikareean) deposition of the Kimberly Member of the upper John Day Formation. Soil column lithological symbols are as for Fig. 3.

xeric moisture regime, whereas the Great Plains is ustic (following terminology of Soil Survey Staff, 1999). The early Miocene may have been not only a dry phase following the aridity of the Oligocene–Miocene boundary, but also a regional transition between Oligocene ustic moisture regimes and Miocene to modern xeric moisture regimes. Such differences in available summer moisture would have led to substantial changes in vegetation, and in the capacity of vegetation to mitigate soil erosion.

5.2. Early Miocene advent of short sod grassland

Crumb-structured paleosols (Patu and Iscit) of the Hemingfordian beds (early Miocene, ca. 19 Ma) in Johnson Creek are the geologically oldest,

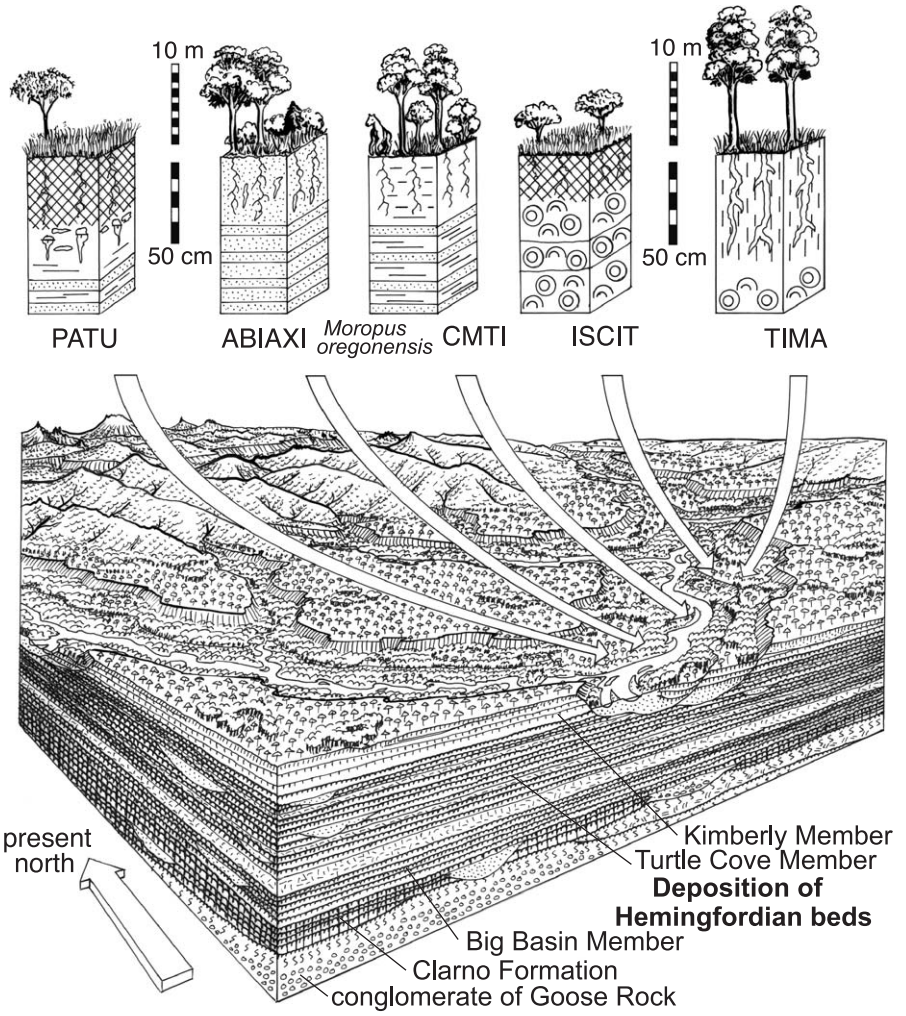

Fig. 21. A reconstruction of Longview Ranch during early Miocene (Hemingfordian) deposition of the Rose Creek Member of the upper John Day Formation. Soil column lithological symbols are as for Fig. 3.

likely sod grassland paleosols (Mollisols) currently known in Oregon (Retallack, 1997a). The silica and shallow carbonate horizons of these paleosols are evidence for a dry climate (< 400 mm mean annual precipitation). This and the shallow fossilized rooting depth indicates that these were short grasslands. Similar evidence from North American paleosols indicates that early and middle Miocene grasslands were confined to semiarid regions until the advent of Mollisols with deep calcic horizons at about 7 Ma, representing the earliest tall grasslands (Retallack, 1997a, 2001a; Retallack et al., 2002).

An early Miocene age of short sod grasslands in Oregon is compatible with increased abundance of grass pollen in rocks of that age in the Pacific Northwest (Leopold et al., 1992). Phytoliths of open-habitat grasses become more abundant at this time in the Great Plains (Strömberg, 2002, this volume), but have not yet been studied in Oregon. Sod grassland interpretation is also compatible with a continent-wide adaptive radiation of hypsodont parahippine horses (MacFadden and Hulbert, 1988), known to have been grazers from tooth morphology and wear (MacFadden, 2000; Janis et al., 2002;

Solounias and Semprebon, 2002). The new grazing fauna of parahippine horses is also known in Hemingfordian rocks of Oregon (Woodburne and Robinson, 1977).

The first appearance of sod grasslands in Oregon at 19 Ma is associated with dry climate, but the grassland paleosols are stratigraphically higher than desertic paleosols (Plas and Plaspa) and below silcrete paleosols of wetter climate higher in the sequence (Figs. 5 and 8). Within the paleosol sequence of the Great Plains, the earliest sod grassland paleosols of the basal Anderson Ranch Formation, also now dated at 19 Ma (MacFadden and Hunt, 1998), are above desertic shallow-calcic paleosols of the upper Harrison Formation (Eagle Crags locality; Retallack, 1990), and among deeper calcic paleosols of the Anderson Ranch Formation (Agate locality; Retallack, 1997a). Both Oregon and Great Plains sequences were coeval with a wet paleoclimatic inflection, with summer-dry seasonality in Oregon and summer-wet seasonality in Nebraska. This was one of numerous wet–dry cycles (Schultz and Stout, 1981; Martin, 1994), and it is unclear why this particular sequence of the early Hemingfordian (19 Ma), and not earlier or later paleoclimate cycles, was the one to introduce sod grasslands. Such climatic volatility is on time scales shorter than likely orographic development of rain shadows (Kohn et al., 2002), although these would exacerbate local climatic variation. Neither the 19 nor 17 Ma arid phases were as dry as the one at the Oligocene–Miocene boundary (23.2 Ma), judging from the Great Plains paleosol record (Retallack, 1997a). Thus, it seems unlikely that climatic drying or seasonality by itself introduced grasslands.

Other explanations for grassland origins have included lower atmospheric carbon dioxide, thus favoring plants with C_4 photosynthetic pathways such as tropical grasses (Cerling et al., 1997). However, carbon isotopic studies of fossil grasses and grazers indicate that early grasslands in both tropical and temperate regions were mostly C_3 before 3 Ma in the Great Plains (Fox and Koch, 2003, this volume), but before 7 Ma elsewhere (MacFadden, 2000). The lack of global synchroneity in expansion of C_4 grasslands argues for local rather than global atmospheric causes (Fox and Koch, 2003). Fire is a physical force promoting grasslands, because trees are destroyed by fire, but grasses sprout again from undamaged rhizomes (Vogl, 1974). However, no charcoal was seen in early Miocene paleosols of either Nebraska or Oregon, despite its abundance in Miocene paleosols elsewhere (Retallack, 1991; Morley and Richards, 1993). Broad plains have been thought to promote grasslands by allowing the free movement of fire and herds of ungulates, but both the Great Plains and Oregon sequences were extensively dissected by erosional valleys during the early Miocene, compared with laterally extensive volcanic ashes and sedimentary facies in underlying Oligocene rocks (Retallack, 1983; Retallack et al., 2000).

The explanation favored here for the origin of this new ecosystem is grass-grazer coevolution, as suggested by Kowalesvsky (1873). Grasses with their modular, rhizomatous growth, basal leaf meristems, sheathing leaves and protected terminal meristems are better adapted than other plants at withstanding the grazing pressure of large herds of ungulates. Horses and antelope, on the other hand, are uniquely suited by virtue of their high crowned teeth, hooves and elongate limbs to life on the open plains. Large herbivores such as rhinos and elephants are particularly destructive of trees, stripping their bark and toppling their trunks (Retallack, 2001a). By this view, grassland sod evolved as a group of adaptations in roots and shoots to withstand increasingly effective trampling and grazing by mammals. Against a near-chaotic background of mountain uplift, sea level change and paleoclimatic oscillation, sod–grassland ecosystems appeared and stayed in semiarid regions of Oregon.

Acknowledgements

I thank Russell Hunt, Jonathan Wynn, Nathan Sheldon, Ted Fremd, Chris Schierup, Lia Vella and Scott Foss for assistance during fieldwork, preparation and curation of the fossil collections. Scott Bates, Dave Van Cleve and Rob Williams generously gave permissions and accommodation for our work on Longview Ranch. Finally, Caroline Strömberg drew together the small circle of those interested in ancient grasslands at a symposium in Berkeley in 2001, and diligently edited this manuscript. Work was funded by NSF grant EAR 0000953.

Appendix A
New chemical analyses of paleosols of the upper John Day Formation

Pedon	Hz	m	JD no.	SiO_2	TiO_2	Al_2O_3	FeO	$Fe_2{}_O_3$	MnO	MgO	CaO	Na_2O	K_2O	P_2O_5	LOI	Total	g cm^{-3}	Ba	Nb	Rb	Sr	Zr
Tima	A	623.9	8383	55.57	0.92	13.22	0.32	5.94	0.03	1.42	2.05	1.33	1.19	0.07	17.36	99.53	1.66	268	8	57	184	187
	Bn	623.7	8384	56.73	0.97	13.49	0.32	5.96	0.03	1.54	2.15	1.30	1.05	0.07	15.86	99.60	1.67	322	11	56	203	194
	Bn	623.5	8385	55.11	1.00	13.43	0.32	6.01	0.03	1.53	2.29	1.38	1.07	0.08	16.89	99.25	1.59	315	21	54	215	186
	C	623.2	8386	55.69	1.00	13.89	0.39	5.28	0.04	1.63	2.79	1.50	1.13	0.14	15.40	99.01	1.6	350	14	55	256	194
Tima	Bq	623.0	8387	56.81	0.94	13.89	0.45	4.24	0.09	1.42	2.55	1.62	1.35	0.10	15.26	98.86	1.59	388	23	61	248	217
Tima	Bq	621.5	8388	57.85	0.81	13.64	0.32	4.10	0.04	1.23	2.36	1.63	1.23	0	15.83	99.21	1.59	327	17	60	237	239
Iscit	A	620.3	8354	58.79	0.91	13.51	0.26	5.46	0.04	0.9	1.38	0.57	0.86	0.06	16.79	99.61	1.4	227	18	58	83	243
	Bq	620.1	8355	60.85	0.71	12.97	0.26	4.02	0.03	0.94	1.40	0.84	1.21	0.06	15.90	99.29	1.58	302	11	63	99	187
	Bq	620.0	8356	61.11	0.73	13.04	0.39	4.09	0.04	0.92	1.59	0.97	1.31	0.06	14.73	99.10	1.72	326	22	63	127	197
Patu	A	619.9	8357	56.00	0.68	13.05	0.26	4.09	0.03	1.24	1.58	0.88	1.11	0.05	19.46	98.54	1.68	283	15	56	119	179
	A	619.8	8358	57.39	0.71	13.83	0.32	4.08	0.04	1.40	1.74	0.94	1.07	0.05	17.33	99.00	1.66	261	17	60	130	188
	Bk	619.6	8359	56.27	0.72	13.06	0.39	4.12	0.04	1.25	1.66	1.01	1.24	0.06	18.09	98.06	1.63	318	14	60	130	200
	C	619.3	8360	56.98	0.71	13.24	0.32	4.12	0.04	1.32	1.75	1.06	1.30	0.07	18.15	99.18	1.65	290	21	66	140	219
Tima	Bn	613.6	8378	53.72	0.88	14.41	0.19	5.47	0.04	1.32	2.26	1.43	1.35	0.05	17.77	99.00	1.85	330	13	66	213	208
Patu	A	612.5	8364	56.32	0.86	13.24	0.13	6.45	0.05	1.34	1.64	0.96	1.30	0.05	16.98	99.42	1.66	423	19	64	121	195
	A	612.4	8365	55.12	0.95	13.74	0.13	6.95	0.04	1.32	1.78	1.09	1.43	0.05	16.47	99.18	1.66	446	15	68	145	204
	Bk	612.3	8366	55.24	0.89	13.79	0.19	6.75	0.04	1.42	1.82	0.90	1.34	0.05	16.64	99.18	1.62	428	15	68	137	206
	C	612.2	8367	67.09	0.41	8.85	0.13	3.67	0.02	0.89	1.14	0.46	0.77	0.04	15.62	99.16	1.38	277	10	53	68	135
Abi.	A	612.1	8368	55.59	0.93	13.67	0.45	5.43	0.05	1.15	2.33	1.65	1.82	0.08	15.32	98.64	1.63	691	12	76	218	188
	C	612.0	8369	57.02	0.94	13.91	0.39	5.19	0.06	1.17	2.38	1.59	1.74	0.09	14.11	98.76	1.64	751	19	76	233	201
	C	611.8	8370	62.72	0.50	10.53	0.19	4.35	0.03	1.24	1.25	0.55	0.91	0.03	15.94	98.32	1.58	243	15	62	76	156
Patu	A	611.0	8371	56.86	0.84	13.56	0.39	5.94	0.06	1.36	2.56	1.64	1.74	0.06	13.80	99.00	1.71	888	12	70	263	205
	A	610.8	8372	57.50	0.87	13.46	0.45	4.97	0.05	1.30	2.62	1.77	1.83	0.06	13.80	98.89	1.7	891	16	73	272	209
	Bk	610.6	8373	56.59	0.82	13.27	0.45	5.55	0.05	1.27	2.58	1.75	1.77	0.06	14.73	99.08	1.71	891	18	71	259	201
	C	610.3	8374	57.60	0.91	13.92	0.58	3.79	0.06	1.11	3.13	2.13	1.83	0.17	13.37	98.81	1.71	871	20	78	297	204
Cmti	A	610.0	8375	54.29	0.85	12.74	0.19	6.76	0.05	1.74	2.62	1.27	1.57	0.20	16.52	98.98	1.63	968	14	65	276	199
	C	609.8	8376	53.86	0.81	13.07	0.26	6.26	0.05	1.63	3.17	1.48	1.68	0.53	15.95	98.94	1.66	972	10	71	255	197
Tima	Bn	583.5	9074	51.47	0.89	15.49	0.26	6.22	0.03	1.39	1.64	0.71	0.94	0.03	19.28	98.46	2.08	278	10	59	125	203
Tima	Bn	573.3	9072	57.53	0.79	13.24	0.45	3.88	0.06	1.30	2.70	1.28	1.45	0.35	16.39	99.58	1.67	427	13	64	225	194
Tima	Bn	569.2	9070	54.59	1.04	15.34	0.45	5.05	0.07	1.17	2.56	1.68	1.14	0.05	16.82	100.11	1.88	426	11	50	249	226
Tima	Bn	552	9069	54.02	0.83	14.66	0.26	5.62	0.08	1.52	2.30	1.30	1.09	0.16	18.49	100.43	1.89	262	13	55	185	247
Tima	Bn	545.3	9067	53.80	0.98	14.34	0.32	6.89	0.07	1.68	2.67	1.85	1.16	0.08	15.80	99.77	1.88	347	10	49	235	195
Plas	AB	537.6	9066	59.22	0.82	13.99	0.51	4.61	0.07	1.19	2.56	1.95	1.62	0.11	13.18	100.00	1.74	438	16	69	234	198
Plas	AB	526.3	9065	59.80	0.82	13.98	0.64	4.61	0.11	1.11	3.17	2.03	1.86	0.45	11.23	100.00	1.76	560	16	72	249	194
Plas	AB	516.2	9064	58.59	0.80	13.73	0.71	4.53	0.10	1.27	2.45	1.96	1.75	0.09	13.21	99.38	1.74	498	11	70	209	207
Plas	AB	502.3	9063	59.56	0.79	13.43	0.71	4.51	0.08	1.36	2.56	2.25	1.86	0.22	12.62	100.14	1.74	546	13	71	187	199
Plas	AB	495	9088	57.94	0.80	13.05	0.64	5.04	0.11	1.31	2.82	2.06	1.75	0.16	13.17	99.00	1.73	441	15	70	199	193
Plas	AB	482.7	9087	58.71	0.90	14.15	0.84	5.35	0.12	1.19	3.09	2.23	1.99	0.12	10.40	99.29	1.78	537	7	74	238	192
Plas	AB	471.3	9086	60.97	0.78	14.00	0.71	4.16	0.08	1.22	2.88	2.29	1.89	0.22	10.93	100.30	1.71	449	13	71	228	209
Plas	AB	447.4	9084	56.15	0.90	13.63	0.68	4.75	0.08	2.62	2.42	2.92	1.63	0.09	14.37	100.45	1.76	400	12	60	191	208
Plas	AB	432.6	9083	54.72	0.89	13.31	0.51	5.14	0.07	1.84	2.51	3.11	1.66	0.09	15.61	99.60	1.64	330	15	70	159	216
Plas	AB	421.2	9082	56.24	0.86	13.46	0.71	5.00	0.08	1.83	2.99	2.75	1.74	0.13	13.56	99.54	1.71	366	17	75	180	215

Plas	AB	411.2	9081	57.51	0.76	13.91	0.64	4.18	0.10	1.70	2.07	2.97	1.72	0.06	13.85	99.64	1.92	431	15	78	184	240
Plas	AB	398.8	9080	56.80	0.92	13.73	1.09	5.21	0.10	1.82	3.13	3.15	1.48	0.24	12.66	100.56	1.86	420	10	64	189	200
Xaxus	AB	387.4	9079	56.53	0.83	13.05	0.71	5.46	0.11	1.96	2.32	2.68	1.65	0.12	14.35	99.93	1.88	338	14	63	145	192
Yapas	AB	373.6	9078	55.70	0.90	14.08	0.06	6.30	0.09	1.29	2.67	3.59	1.47	0.08	13.40	99.74	1.84	468	11	60	261	223
Yapas	AB	357.5	9077	56.52	0.72	13.41	0.39	4.66	0.07	0.95	2.17	3.95	2.42	0.10	14.96	100.44	1.91	412	14	90	184	195
Xaxus	AB	344.6	9076	61.61	0.48	11.73	0.51	3.51	0.05	0.86	2.16	3.38	2.16	0.11	12.74	99.50	2.05	254	15	70	179	117
Xaxus	AB	334.8	9075	61.50	0.61	11.37	0.61	3.22	0.06	0.79	3.15	3.43	1.66	0.11	12.69	99.31	2.08	371	13	67	199	168
Yapas	AB	321.9	9192	56.99	0.77	13.21	0.77	4.77	0.08	1.33	2.86	1.88	1.74	0.25	13.21	98.04	1.82	429	11	68	182	188
Plas	AB	311.5	9191	56.53	0.77	13.02	0.77	4.96	0.12	1.56	2.68	1.70	1.61	0.16	15.43	99.49	1.81	425	9	56	166	193
Plas	AB	297.6	9190	58.71	0.78	14.17	0.64	5.3	0.09	1.24	3.05	2.21	1.83	0.07	11.26	99.52	1.81	518	11	73	227	212
Plas	AB	282.2	9189	58.85	0.83	13.95	0.58	4.95	0.10	1.59	3.21	2.25	1.35	0.16	11.94	99.92	1.74	441	11	61	211	197
Pla'pa	A	276.7	8396	55.96	0.83	12.66	0.51	5.36	0.16	1.77	3.24	1.88	1.38	0.33	14.86	99.10	1.76	462	17	60	200	188
	A	276.5	8397	57.83	0.86	13.13	0.64	4.56	0.14	1.66	3.19	1.98	1.55	0.33	13.31	99.33	1.75	456	15	63	204	199
	A	276.4	8398	56.85	85	12.89	0.58	4.97	0.25	1.71	3.28	1.97	1.46	0.34	14.10	99.41	2.36	503	20	64	204	197
	Bk	276.2	8399	33.28	0.45	6.52	0.71	3.96	0.2	1.05	24.9	1.23	1.19	0.18	25.44	99.28	1.72	260	5	29	130	86
Plas	A	276.1	8400	55.83	0.84	12.64	0.64	5.40	0.11	1.75	2.97	1.83	1.43	0.17	15.29	99.06	1.69	422	18	61	189	188
	A	276.0	8401	57.61	0.87	13.10	0.58	4.67	0.11	1.73	3.19	1.89	1.47	0.20	14.13	99.72	1.71	468	18	67	197	195
	A	275.8	8402	57.35	0.86	12.98	0.51	4.50	0.1	1.65	3.31	1.88	1.48	0.26	14.24	99.30	1.71	457	17	64	200	195
	A	275.7	8403	55.45	0.84	12.62	0.64	4.75	0.09	1.69	3.21	1.81	1.4	0.22	16.22	99.10	1.68	420	13	56	191	187
	Bk	275.6	8404	31.81	0.41	6.20	0.58	4.27	0.44	0.99	26.0	1.13	1.27	0.29	25.95	99.45	1.41	333	5	5	5	5
Pla'pa	A	275.4	8405	54.96	0.81	12.45	0.58	4.46	0.1	1.66	3.01	1.87	1.47	0.24	17.55	99.32	1.69	448	8	59	192	189
Plas	AB	268.6	8394	54.20	0.87	12.74	0.39	5.93	0.08	2.23	3.01	1.65	1.09	0.11	16.64	99.08	1.79	349	12	51	176	169
Plas	AB	259.5	8393	54.48	0.84	13.39	0.32	5.88	0.09	2.12	3.48	1.81	1.16	0.12	15.24	99.04	1.77	329	13	58	189	163
Plas	AB	249.5	8392	54.45	0.78	12.66	0.32	5.84	0.09	2.11	2.84	1.67	1.09	0.07	17.69	99.73	1.87	312	16	60	154	207
Plas	AB	240.8	8391	55.18	0.88	12.98	0.39	5.86	0.08	1.92	3.11	1.99	0.99	0.1	15.66	99.25	1.79	331	15	50	173	193
Tuff	–	229.5	8389	56.03	0.99	13.35	0.00	4.51	0.06	1.93	3.55	1.84	1.38	0.2	14.90	98.87	1.83	667	13	55	314	180
Xaxus	AB	219.5	8423	56.76	0.79	13.28	0.71	5.23	0.07	1.62	3.17	2.47	2.51	0.3	12.37	99.50	2.15	651	13	91	390	206
Xaxus	AB	206.0	8422	56.21	0.82	13.03	0.51	5.54	0.1	1.73	3.43	2.78	1.81	0.13	12.95	99.20	1.99	461	13	57	300	195
Ya'pa	AB	191.0	8421	55.44	1.03	13.46	0.96	5.97	0.11	1.88	3.72	2.74	1.90	0.14	11.86	99.42	2.02	461	10	71	289	178
TRT	–	178.0	8407	60.27	0.41	12.20	0.32	3.28	0.06	0.82	2.36	3.69	1.86	0.14	13.25	98.81	1.74	510	17	59	256	223
Xaxus	AB	165.0	8419	57.56	0.81	11.69	0.58	5.88	0.09	1.45	3.05	3.05	1.82	0.13	12.95	99.19	2.04	357	10	59	191	161
Xa'pa	AB	147.6	8418	55.52	1.01	13.15	1.03	6.42	0.13	1.79	3.84	2.85	1.52	0.20	12.61	100.26	2.13	372	8	50	209	170
Xaxus	AB	147.0	8417	56.61	0.89	13.19	0.84	5.83	0.11	1.61	3.50	2.99	1.42	0.09	12.65	99.92	2.06	397	10	49	214	216
Xaxus	AB	130.6	8416	56.57	0.98	12.85	1.09	6.40	0.16	1.74	3.67	3.12	1.76	0.10	10.94	99.58	2.06	354	11	60	209	169
Xa'pa	AB	113.0	8415	58.92	0.79	12.51	0.84	4.92	0.11	1.14	3.18	3.22	1.87	0.09	11.45	99.24	2.05	467	11	81	219	168
Xa'pa	AB	99.0	8410	51.57	0.79	11.41	0.84	4.40	0.23	1.24	7.93	3.07	1.47	0.25	15.62	99.00	2.01	409	10	56	198	153
Xaxus	AB	88.0	8409	55.78	1.01	13.22	0.77	6.66	0.15	1.83	3.86	2.82	1.52	0.16	11.25	99.20	2.08	411	14	60	213	200
Xaxus	AB	68.0	8408	56.25	1.05	13.64	1.16	6.34	0.16	1.91	3.54	2.69	2.06	0.11	10.48	99.63	2.14	432	14	73	201	225
DCT	–	65.0	8406	61.58	0.14	12.10	0.13	2.22	0.05	0.32	2.54	3.81	0.65	0.03	15.83	99.54	1.52	556	63	42	162	393
Xaxus	AB	54.5	8431	56.87	0.86	13.14	0.84	5.59	0.12	1.43	2.91	2.75	2.29	0.09	12.69	99.77	2.1	526	13	81	193	217
Xaxus	AB	43.5	8429	57.79	0.75	13.17	0.51	4.91	0.09	1.27	2.83	3.26	1.77	0.13	13.72	100.36	2.08	451	18	62	185	222
Xaxus	AB	34.5	8428	54.72	0.88	13.26	0.58	5.53	0.10	1.48	3.41	2.82	1.53	0.37	14.43	99.25	2.13	432	18	55	188	199
Xaxus	AB	24.0	8427	55.01	0.91	12.90	0.71	5.79	0.19	1.65	3.15	2.72	2.17	0.17	13.43	98.99	2.12	537	14	78	198	222
Xaxus	AB	13.0	8426	57.16	0.85	13.28	0.64	5.64	0.12	1.52	2.98	2.91	2.10	0.11	12.70	100.20	1.96	548	18	74	188	223
Error	± 1σ	–	–	0.77	.044	0.23	–	0.20	.001	0.04	0.04	0.05	0.02	.015	–	–	0.07	50	3	7	0.6	0.6

References

Albright, L.B., Fremd, T.J., Swisher, C.C., MacFadden, B.J., 2001. Toward a revision of the chronostratigraphy of the John Day Formation, Oregon. Paleobios 21 (Suppl. to no. 2), 22.

Alroy, J., 2000. New methods for quantifying macroevolutionary patterns and processes. Paleobiology 26, 707–733.

Barley, K.P., 1959. Earthworms and soil fertility: IV. The influence of earthworms on the physical properties of a red brown earth. Aust. J. Agric. Res. 10, 371–376.

Beadle, N.C.W., 1981. The Vegetation of Australia. Cambridge Univ. Press, London.

Bestland, E.A., 2000. Weathering flux and CO_2 consumption determined from paleosol sequences across the Eocene–Oligocene transition. Palaeogeogr. Palaeoclimatol. Palaeoecol. 156, 301–326.

Bestland, E.A., Swisher, C.C., 1996. Milankovitch-scale climate cycles recorded in Oligocene paleosols from central Oregon. Abstr. Programs-Geol. Soc. Am., Cordilleran Sect. Ann. Meet. 28, 49.

Birnbaum, S.J., Wireman, J.W., Borowski, R., 1986. Silica precipitation induced by anaerobic sulfate-producing bacterium *Desulfovibrio desulfuricans*: effects upon cell morphology and implications for preservation. In: Crick, R.E. (Ed.), Origin, Evolution and Modern Aspects of Biomineralization in Plants and Animals. Plenum, New York, pp. 507–526.

Blinnikov, M., Busacca, A., Whitlock, C., 2002. Reconstruction of the late Pleistocene grassland of the Columbia Basin, Washington. Palaeogeogr. Palaeoclimatol. Palaeoecol. 177, 77–101.

Bown, T.M., 1982. Ichnofossils and rhizoliths of the nearshore Jebel Qatrani formation (Oligocene), Fayum Province, Egypt. Palaeogeogr. Palaeoclimatol. Palaeoecol. 40, 255–309.

Bown, T.M., Kraus, M.J., 1983. Ichnofossils of the alluvial Willwood Formation (Lower Eocene), Bighorn Basin, northwest Wyoming, U.S.A. Palaeogeogr. Palaeoclimatol. Palaeoecol. 43, 95–128.

Brewer, R., 1976. Fabric and Mineral Analysis of Soils, 2nd ed. Krieger, New York.

Bryant, H.N., 1996. Nimravidae. In: Prothero, D.R., Emry, R.J. (Eds.), The Terrestrial Eocene–Oligocene Transition in North America. Cambridge Univ. Press, Cambridge, pp. 453–475.

Busacca, A., 1999. Dust Aerosols, Loess Soils and Global Change: Field Tour. Washington State University, Pullman.

Cande, S.C., Kent, D.V., 1992. A new geomagnetic polarity time scale for the late Cretaceous and Cenozoic. J. Geophys. Res. 97, 13917–13951.

Cerling, T.E., MacFadden, B.J., Leakey, M.G., Quade, J., Eisenmann, V., Ehleringer, R., 1997. Global vegetation changes through the Miocene–Pliocene boundary. Nature 389, 153–158.

Chadwick, O.A., Hendricks, D.M., Nettleton, W.D., 1987. Silica in duric soils: I. A depositional model. Soil Sci. Soc. Am. J. 51, 975–982.

Chadwick, O.A., Nettleton, W.D., Staidle, G.J., 1995. Soil polygenesis as a function of Quaternary climate change, northern Great Basin, USA. Geoderma 68, 10–26.

Chaney, R.W., 1925. Notes on Two Fossil Hackberries from the Tertiary of the Western United States. Carnegie Inst. Washington Publ. 349, 51–56.

Chartres, C.J., Norton, L.D., 1993. Micromorphological and chemical properties of Australian soils with hardsetting and duric horizons. In: Ringrose-Voase, A.J., Humphreys, G.S. (Eds.), Soil Micromorphology. Developments in Soil Science, vol. 22, pp. 825–834.

Coombs, M.C., 1978. Reevaluation of early Miocene North American *Moropus* (Perissodactyla, Chalicotheriidae, Schizotheriinae). Bull. Carnegie Mus. Nat. Hist. 4, 1–62.

Coombs, M.J., Hunt, R.M., Stepleton, E., Albright, L.B., Fremd, T.J., 2001. Stratigraphy, chronology, biogeography and taxonomy of early Miocene small chalicotheres in North America. J. Vertebr. Paleontol. 21, 607–620.

Creutzberg, D., Kauffman, J.H., Bridges, E.M., del Fossa, G.M., 1990. Micromorphology of "cangahua": a cemented subsurface horizon in soils from Ecuador. In: Douglas, L.A. (Ed.), Soil Micromorphology: A Basic and Applied Science. Elsevier, Amsterdam, pp. 367–372.

Darwin, C., 1872. The Descent of Man, and Selection in Relation to Sex. John Murray, London.

Darwin, C., 1896. The Formation of Vegetable Mould through the Action of Worms, with Observations on their Habits. Appleton, New York.

DeLancey, S., Genetti, C., Rude, N., 1988. Some Sahaptian–Klamath–Tsimshianic lexical sets. In: Shipley, W. (Ed.), In Honor of Mary Haas. Mouton de Gruyter, Berlin, pp. 195–224.

Dingus, L., 1990. Systematics, stratigraphy and chronology for mammalian fossils (late Arikareean to Hemingfordian) from the uppermost John Day Formation, Warm Springs, Oregon. Paleobios 12, 1–24.

Downing, K.F., Park, L.E., 1998. Geochemistry and early diagenesis of mammal-bearing concretions from the Sucker Creek Formation (Miocene) of southeastern Oregon. Palaios 13, 14–27.

Dugas, D.P., Retallack, G.J., 1993. Middle Miocene fossil grasses from Fort Ternan, Kenya. J. Paleontol. 67, 113–128.

Duringer, P., Brunet, P., Cambefort, Y., Beauvillain, A., Mackaye, H.T., Vignaud, P., Schuster, M., 2000. Des Boules des bousiers fossiles et leurs terriers dans les sites à Australopithèques du Pliocène Tchadien. Bull. Soc. Geol. Fr. 171, 259–269.

FAO (Food and Agriculture Organization), 1974. Soil map of the world. Legend, vol. I. UNESCO, Paris.

FAO (Food and Agriculture Organization), 1975a. Soil map of the world. North America, vol. II. UNESCO, Paris.

FAO (Food and Agriculture Organization), 1975b. Soil map of the world. Mexico and Central America, vol. III. UNESCO, Paris.

Fisher, R.V., Rensberger, J.M., 1972. Physical stratigraphy of the John Day Formation, central Oregon. Univ. Calif. Publ. Geol. Sci. 101, 1–45.

Flores-Román, D., Alcalá-Martínez, J.R., González-Velazquez, A., Gama-Castro, J.E., 1996. Duripans in subtropical and temperate subhumid climate of the trans-Mexico Volcanic belt. Rev. Mex. Cienc. Geol. 13, 228–239.

Foss, S.E., Fremd, T., 2001. Biostratigraphy of the Entelodontidae (Mammalia, Artiodactyla). Paleobios 21 (Suppl. to no. 2), 53.

Fox, D.L., Koch, P.L., 2003. Tertiary history of C_4 biomass in the Great Plains, USA. Geology 31, 809–812.

Fox, D.L., and Koch, P.L., this volume. Carbon and oxygen isotopic variability in Neogene paleosol carbonates: constraints on the evolution of the C_4-grasslands of the Great Plains, USA. Palaeogeogr. Palaeoclimatol. Palaeoecol. (in press).

Fremd, T., 1988. Assemblages of fossil vertebrates in pre-ignimbrite deposits of the Turtle Cove Member, John Day Formation (Arikareean), from outcrops within the Sheep Rock Unit, John Day Fossil Beds National Monument. J. Vertebr. Paleontol. 8, A15 (Abstr.).

Fremd, T., 1991. Early Miocene mammalian populations from Turtle Cove, Oregon. J. Vertebr. Paleontol. 11, A29 (Abstr.).

Fremd, T., 1993. Refinement of spatial and temporal distributions of biotas within the volcaniclastic sequences of the John Day Basin. J. Vertebr. Paleontol. 13, A36 (Abstr.).

Fremd, T., Bestland, E.A., Retallack, G.J., 1994. John Day Basin Field Trip Guide and Road Log for the Society of Vertebrate Paleontology Annual Meeting. Northwest Interpretive Association, Seattle.

Genise, J.F., Mángano, M.G., Buatois, L.A., Laza, J.H., Vered, M., 2000. Insect trace fossil associations in paleosols: the *Coprinisphaera* ichnofacies. Palaios 15, 49–64.

Gile, L.H., Hawley, J.W., Grossman, J.B., 1981. Soils and geomorphology in the Basin and Range area of southern New Mexico—guidebook to the Desert Project. Mem. N. M. Bur. Mines Miner. Resour. 39.

Hanna, G.D., 1920. Fossil mollusks from the John Day Basin in Oregon. Univ. Or. Publ. 1 (6), 1–8.

Hanna, G.D., 1922. Freshwater mollusks from Oregon contained in the Condon Museum. Univ. Or. Publ. 1 (12), 1–12.

Hay, O.P., 1908. The Fossil Turtles of North America. Carnegie Inst. Washington Publ. 75, 1–568.

Hay, R.L., 1963. Stratigraphy and zeolitic diagenesis of the John Day Formation of Oregon. Univ. Calif. Publ. Geol. Sci. 42, 199–261.

Honey, J.G., Harrison, T.A., Prothero, D.R., Stevens, M.S., 1998. Camelidae. In: Janis, C.M., Scott, K.M., Jacobs, L.L. (Eds.), Evolution of Tertiary Mammals of North America. Terrestrial Carnivores, Ungulates and Ungulatelike Mammals, vol. 1. Cambridge Univ. Press, Cambridge, pp. 439–462.

Hunt, R.M., 2002. New amphycyonid carnivorans (Mammalia, Daphoeninae) from the early Miocene of southeastern Wyoming. Am. Mus. Novit. 3385, 1–41.

Hunt, R.M., Stepleton, E., 2001. Geology and paleontology of the upper John Day beds, John Day River Valley, Oregon. Lithostratigraphic and biochronologic subdivision in the Haystack Valley and Kimberly areas. Paleobios 21 (Suppl. to no. 2), 69.

Jacobs, B.F., Kingston, J.D., Jacobs, L.L., 1999. The origin of grass-dominated ecosystems. Ann. Mo. Bot. Gard. 86, 590–643.

Janis, C.M., 2000. Victors by default: the mammalian succession. In: Gould, S.J. (Ed.), The Book of Life. W.W. Norton, New York, pp. 169–212.

Janis, C.M., Damuth, J., Theodore, J.M., 2002. The origins and evolution of the North American grassland biome: the story from the hoofed mammals. Palaeogeogr. Palaeoclimatol. Palaeoecol. 177, 183–198.

Jermann, T.M., Opitz, J.G., Stackhouse, J., Benner, S.A., 1995. Reconstructing the evolutionary history of the artiodactyl ribonuclease superfamily. Nature 374, 57–59.

Jones, B., Renault, B.W., Rosen, M.R., Klyen, L., 1998. Primary siliceous rhizoliths from the Loop Road Hot Springs, North Island, New Zealand. J. Sediment. Res. 68, 115–123.

Joshi, N.V., Kelkar, B.V., 1952. The role of earthworms in soil fertility. Indian J. Agric. Sci. 22, 189–196.

Koch, P., 1998. Isotopic reconstruction of past continental environments. Annu. Rev. Earth Planet. Sci. 26, 573–613.

Kohn, M., Miselis, J., Fremd, T.J., 2002. Oxygen isotope evidence for progressive uplift of the Cascade Range Oregon. Earth Planet. Sci. Lett. 204, 1–15.

Korth, W.W., 1994. The Tertiary Record of Rodents in North America. Plenum, New York.

Kowalesvsky, V., 1873. Sur l' *Anchitherium aurelianense* Cuv., et sur l'histoire paleontologique des chevaux. Mém. Acad. Imp. Sci. St.-Pétersbg. 20, 1–73.

Lander, B., 1998. Oreodontoidea. In: Janis, C.M., Scott, K.M., Jacobs, L.L. (Eds.), Evolution of Tertiary Mammals of North America. Terrestrial Carnivores, Ungulates and Ungulatelike Mammals, vol. 1. Cambridge Univ. Press, Cambridge, pp. 402–425.

Leopold, E.B., Denton, M.F., 1987. Comparative age of grassland and steppe east and west of the Rocky Mountains. Ann. Mo. Bot. Gard. 74, 841–867.

Leopold, E.B., Liu, G.-W., Clay-Poole, S., 1992. Low biomass vegetation in the Oligocene? In: Prothero, D.R., Berggren, W.A. (Eds.), Eocene–Oligocene Climatic and Biotic Evolution. Princeton Univ. Press, Princeton, pp. 399–420.

Lull, R.S., 1921. New camels in the Marsh Collection. Am. J. Sci. 5, 392–404.

MacFadden, B.J., 1998. Equidae. In: Janis, C.M., Scott, K.M., Jacobs, L.L. (Eds.), Evolution of Tertiary Mammals of North America. Terrestrial Carnivores, Ungulates and Ungulatelike Mammals, vol. 1. Cambridge Univ. Press, Cambridge, pp. 537–559.

MacFadden, B.J., 2000. Origin and evolution of the grazing guild in Cenozoic New World mammals. In: Sues, H.D. (Ed.), Evolution of Herbivory in Terrestrial Verterbates: Perspectives from the Fossil Record. Cambridge Univ. Press, Cambridge, pp. 223–243.

MacFadden, B.J., Hulbert, R.C., 1988. Explosive speciation at the base of the adaptive radiation of Miocene grazing horses. Nature 336, 466–468.

MacFadden, B.J., Hunt, R.M., 1998. Magnetic polarity stratigraphy and correlation of the Arikaree Group, Arikareean (late Oligocene–early Miocene) of northwestern Nebraska. In: Terry, D.O., La Garry, H.E., Hunt, R.M. (Eds.), Depositional Environments, Lithostratigraphy, and Biostratigraphy of the White River and Arikaree Groups (Late Eocene to Early Miocene, North America). Spec. Pap.-Geol. Soc. Am., vol. 325, pp. 143–165.

Mack, G.H., James, W.C., Monger, H.C., 1993. Classification of paleosols. Bull. Geol. Soc. Am. 105, 129–136.

Martin, L.D., 1994. Cenozoic climatic history from a biological perspective. TER-QUA Symp. Ser. 2, 39–56.

Merriam, J.C., Sinclair, W.J., 1906. Tertiary faunas of the John Day region. Univ. Calif. Publ. Geol. Sci. 5, 171–205.

Morley, R.J., Richards, K., 1993. Graminaceae cuticle, key indicator of late Cenozoic climate change in the Niger Delta. Rev. Palaeobot. Palynol. 77, 119–127.

Murphy, C.P., 1983. Point counting pores and illuvial clay in thin sections. Geoderma 31, 133–140.

Northcote, K.H., 1974. A Factual Key for the Recognition of Australian Soils. Rellim, Adelaide.

O'Geen, A.T., Busacca, A.J., 2001. Faunal burrows as indicators of palaeovegetation in eastern Washington. Palaeogeogr. Palaeoclimatol. Palaeoecol. 169, 23–37.

Oleschko, K., 1990. Cementing agents: morphology and its relation to the nature of "tepetates". In: Douglas, L.A. (Ed.), Soil Micromorphology: A Basic and Applied Science. Elsevier, Amsterdam, pp. 381–386.

Orr, E.L., Orr, W.N., 1998. Oregon Fossils. Kendall-Hunt, Dubuque, IA.

Osborn, H.F., 1918. Equidae of the Oligocene, Miocene and Pliocene of North America: iconographic type revision. Mem. Am. Mus. Nat. Hist. 2, 1–326.

Pauw, A., Johnson, S., 1999. Table Mountain: A Natural History. Fernwood Press, Vlaeberg, South Africa.

Pawluk, S., Bal, L., 1985. Micromorphology of selected mollic epipedons. In: Douglas, L.A., Thompson, M.L. (Eds.), Soil Micromorphology and Soil Classification. Soil Sci. Soc. Am. Spec. Publ., vol. 15, pp. 63–83.

Pierce, H.G., 1992. The non-marine molluscs of the late Oligocene–early Miocene Cabbage Patch fauna of western Montana: II. Terrestrial gastropod families other than Pupillidae (Pulmonata, Stylommatophora). J. Paleontol. 66, 610–620.

Pilsbry, H.A., 1939–48. Land Mollusca of North America north of Mexico. 2 vols. Mon. Acad. Nat. Sci. Philadelphia 3, 2 vols, 1–994 and 1–1113.

Prothero, D.R., 1996. Camelidae. In: Prothero, D.R., Emry, R.J. (Eds.), The Terrestrial Eocene–Oligocene transition in North America. Cambridge Univ. Press, Cambridge, pp. 609–651.

Prothero, D.R., Rensberger, J.M., 1985. Preliminary magnetostratigraphy of the John Day Formation, Oregon, and the North American Oligocene–Miocene boundary. Newsl. Stratigr. 15, 59–70.

Rensberger, J.M., 1971. Entoptychine pocket gophers (Mammalia, Geomyoidea) of the early Miocene, John Day Formation, Oregon. Univ. Calif. Publ. Geol. Sci. 90, 1–209.

Rensberger, J.M., 1973. Pleurolicine rodents (Geomyoidea) of the John Day Formation, Oregon. Univ. Calif. Publ. Geol. Sci. 102, 1–95.

Rensberger, J.M., 1983. Successions of Meniscomyine and Allomyine rodents (Aplodontidae) in the Oligo–Miocene John Day Formation, Oregon. Univ. Calif. Publ. Geol. Sci. 124, 1–157.

Retallack, G.J., 1983. Late Eocene and Oligocene paleosols from Badlands National Park, South Dakota. Spec. Pap.-Geol. Soc. Am. 193, 1–82.

Retallack, G.J., 1984. Trace fossils of burrowing beetles and bees in an Oligocene paleosol, Badlands National Park, South Dakota. J. Paleontol. 58, 571–592.

Retallack, G.J., 1990. The work of dung beetles and its fossil record. In: Boucot, A.J. (Ed.), Evolutionary Paleobiology of Behavior. Elsevier, Amsterdam, pp. 214–226.

Retallack, G.J., 1991. Miocene Paleosols and Ape Habitats in Pakistan and Kenya. Oxford Univ. Press, New York.

Retallack, G.J., 1993. Classification of paleosols: discussion. Geol. Soc. Amer. Bull. 105, 1635–1637.

Retallack, G.J., 1994a. A pedotype approach to latest Cretaceous and earliest Tertiary paleosols in eastern Montana. Geol. Soc. Amer. Bull. 106, 1377–1397.

Retallack, G.J., 1994b. The environmental factor approach to the interpretation of paleosols. In: Amundson, R., Harden, J., Singer, M. (Eds.), Factors in Soil Formation—A Fiftieth Anniversary Retrospective. Soil Sci. Soc. Am. Spec. Publ., vol. 33, pp. 31–64.

Retallack, G.J., 1997a. Neogene expansion of the North American prairie. Palaios 12, 380–390.

Retallack, G.J., 1997b. A Colour Guide to Paleosols. Wiley, Chichester.

Retallack, G.J., 1998. Fossil soils and completeness of the rock and fossil record. In: Donovan, S.K., Paul, C.R.C. (Eds.), The Adequacy of the Fossil Record. Wiley, Chichester, pp. 131–162.

Retallack, G.J., 2000. Depth to pedogenic carbonate horizon as a paleoprecipitation indicator? Comment. Geology 28, 572.

Retallack, G.J., 2001a. Cenozoic expansion of grasslands and global climatic cooling. J. Geol. 109, 407–426.

Retallack, G.J., 2001b. Soils of the Past. Blackwell, Oxford.

Retallack, G.J., 2002a. Late Oligocene and early Miocene paleosols near Kimberly, Oregon. Unpub. Rept. John Day Fossil Beds National Monument Contract P9325020029.

Retallack, G.J., 2002b. Carbon dioxide and climate over the past 300 Myr. Philos. Trans. R. Soc. Lond. A360, 659–673.

Retallack, G.J., Alonso-Zarza, A.M., 1998. Middle Triassic paleosols and paleoclimate of Antarctica. J. Sediment. Res. 68, 169–184.

Retallack, G.J., Bestland, E.A., Fremd, T.J., 2000. Eocene and Oligocene paleosols of central Oregon. Spec. Pap.-Geol. Soc. Am. 344, 1–192.

Retallack, G.J., Tanaka, S., Tate, T., 2002. Late Miocene advent of tall grassland paleosols in Oregon. Palaeogeogr. Palaeoclimatol. Palaeoecol. 183, 329–354.

Rigsby, B.J., 1965. Linguistic relations in the southern Plateau. PhD thesis, Univ. Oregon, Eugene.

Roth, B., 1986. Land mollusks (Gastropoda, Pulmonata) from the early Tertiary Bozeman Group, Montana. Proc. Calif. Acad. Sci. 49, 237–267.

Royer, D.L., 1999. Depth to pedogenic carbonate horizon as a paleoprecipitation indicator? Geology 27, 1123–1126.

Sapir, E., 1911. Post-positions in Wishram. In: Boas, F. (Ed.), Handbook of American Indian Languages. Bull. Am. Ethnol., vol. 40(1), pp. 650–654.

Schultz, C.B., Falkenbach, C.H., 1947. Merychyinae, a subfamily of oreodonts. Bull. Am. Mus. Nat. Hist. 88, 157–286.

Schultz, C.B., Falkenbach, C.H., 1949. Promerychochoerinae, a new family of oreodonts. Bull. Am. Mus. Nat. Hist. 93, 69–198.

Schultz, C.B., Falkenbach, C.H., 1968. The phylogeny of the oreodonts. Bull. Am. Mus. Nat. Hist. 139. 498 pp.

Schultz, C.B., Stout, M., 1981. Ancient soils and climatic changes in the central Great Plains. Trans. Nebr. Acad. Sci. 8, 187–205.

Sheldon, N.D., Retallack, G.J., 2001. Equation for compaction of paleosols due to burial. Geology 29, 247–250.

Sheldon, N.D., Retallack, G.J., Tanaka, S., 2002. Geochemical climofunctions from North American soils and application to paleosols across the Eocene–Oligocene boundary in Oregon. J. Geol. 110, 687–696.

Sinclair, W.J., 1905. New or imperfectly known rodents and ungulates from the John Day Series. Univ. Calif. Publ. Geol. Sci. 4, 125–143.

Smith, R.M.H., Masin, T.R., Ward, J.R., 1993. Flash-flood sediments and ichnofacies of the Late Pleistocene Homeb Silts, Kuiseb River, Namibia. Sediment. Geol. 85, 579–599.

Soil Survey Staff, 1993. Soil Survey Manual. U.S. Dept Agric. Handbook, vol. 18, pp. 1–437.

Soil Survey Staff, 1999. Keys to Soil Taxonomy. Pocahontas Press, Blacksburg, VA.

Solounias, N., Semprebon, G., 2002. Advances in reconstruction of ungulate ecomorphology with application to early equids. Am. Mus. Novit. 3366, 1–49.

Stace, H.C.T., Hubble, G.D., Brewer, R., Northcote, K.H., Sleeman, J.R., Mulcahy, M.J., Hallsworth, E.G., 1968. A Handbook of Australian Soils. Rellim, Adelaide.

Strömberg, C.A.E., 2002. The origin and spread of grass-dominated ecosystems in the late Tertiary of North America: preliminary results concerning the evolution of hypsodonty. Palaeogeogr. Palaeoclimatol. Palaeoecol. 177, 59–75.

Strömberg, C.A.E., this volume. Using phytolith assemblages to reconstruct the origin and spread of grass-dominated habitats in the Great Plains during the late Eocene to early Miocene. Palaeogeogr. Palaeoclimatol. Palaeoecol.

Tate, T.A., 1998. Micromorphology of loessial soils and paleosols on aggrading landscapes on the Columbia Plateau. MSc Thesis, Washington State Univ., Pullman.

Van Valkenburgh, B., 1991. Iterative evolution of hypercarnivory in canids (Mammalia, Carnivora): evolutionary interactions among sympatric predators. Paleobiology 17, 340–362.

Vogl, R.J., 1974. Effects of fire on grasslands. In: Kozlowski, T.T., Ahlgren, C.E. (Eds.), Fire and Ecosystems. Academic Press, New York, pp. 139–194.

Webb, S.D., 1998. Hornless ruminants. In: Janis, C.M., Scott, K.M., Jacobs, L.L. (Eds.), Evolution of Tertiary Mammals of North America. Terrestrial Carnivores, Ungulates and Ungulatelike Mammals, vol. 1. Cambridge Univ. Press, Cambridge, pp. 463–476.

Wang, X., 1994. Phylogenetic systematics of the Hesperocyoninae (Carnivora, Canidae). Bull. Am. Mus. Nat. Hist. 221, 1–207.

Wang, Y., Cerling, T.E., 1994. A model of fossil tooth and bone diagenesis: implications for paleodiet reconstruction from stable isotopes. Palaeogeogr. Palaeoclimatol. Palaeoecol. 107, 281–289.

Wang, X., Tedford, R.H., Taylor, B.E., 1999. Phylogenetic systematics of the Borophaginae (Carnivora, Canidae). Bull. Am. Mus. Nat. Hist. 243, 1–391.

Weaver, J.E., 1920. Root Development in the Grassland Formation. Carnegie Inst. Washington Publ., vol. 292, pp. 1–151.

Wing, S.L., 1987. Eocene and Oligocene floras and vegetation of the northern Rocky Mountains. Ann. Mo. Bot. Gard. 74, 748–754.

Wing, S.L., 1998. Tertiary vegetation of North America as a context for mammalian evolution. In: Janis, C.M., Scott, K.M., Jacobs, L.L. (Eds.), Evolution of Tertiary Mammals of North America. Terrestrial Carnivores, Ungulates and Ungulatelike Mammals, vol. 1. Cambridge Univ. Press, Cambridge, pp. 37–65.

Woodburne, M.O., Robinson, P.T., 1977. A new late Hemingfordian mammal fauna from the John Day Formation, Oregon, and its stratigraphic implications. J. Paleontol. 51, 750–757.

Wynn, J.G., Retallack, G.J., 2001. Paleoenvironmental reconstruction of middle Miocene paleosols bearing *Kenyapithecus* and *Victoriapithecus*, Nyakach Formation, southwestern Kenya. J. Hum. Evol. 40, 263–288.

Zachos, J., Pagani, M., Sloan, L., Thomas, E., Billups, K., 2001a. Trends, rhythms, and aberrations in global climate 65 Ma to present. Science 292, 689–693.

Zachos, J.C., Shackleton, N.J., Revenaugh, J.S., Pälike, H., Flower, B.P., 2001b. Climate response to orbital forcing across the Oligocene–Miocene boundary. Science 292, 274–278.